Title: Tilting the balance between RNA interference and replication eradicates Leishmania RNA virus 1 and mitigates the inflammatory response.

Authors: Brettmann EA, Shaik JS, Zangger H, Lye LF, Kuhlmann FM, Akopyants NS, Oschwald DM, Owens KL, Hickerson SM, Ronet C, Fasel N, Beverley SM

Journal: Proceedings of the National Academy of Sciences of the United States of America

Year: 2016 Oct 25

Volume: 113

Issue: 43

Pages: 11998-12005

DOI: 10.1073/pnas.1615085113

Sept 20, 2016

Running Title: Elimination of *Leishmania* LRV1 by RNA interference

Classification: Biological sciences - Microbiology

Title:

Tilting the balance between RNA interference and replication eradicates *Leishmania* RNA virus 1 and mitigates the inflammatory response

Authors: Erin A. Brettmann[a], Jahangheer Shaik[a], Haroun Zangger[b], Lon-Fye Lye[a], F. Matthew Kuhlmann[c], Natalia S. Akopyants[a], Dayna M. Oschwald[d,e], Katherine L. Owens[a], Suzanne M. Hickerson[a], Catherine Ronet[b], Nicolas Fasel[b], and Stephen M. Beverley[a, *]

[a]Department of Molecular Microbiology, Washington University School of Medicine, 660 S. Euclid Ave, Campus Box 8230, St. Louis, MO 63110; [b]Dept. of Biochemistry, University of Lausanne, Ch. des Boveresses 155, 1066 Epalinges, Switzerland; [c]Division of Infectious Diseases, Department of Medicine, Washington University School of Medicine, 660 S. Euclid Ave, Campus Box 8230, St. Louis, MO 63110; [d,e]Genome Technology Access Center, Washington University.

*Corresponding author: S. M. Beverley, stephen.beverley@wustl.edu; Department of Molecular Microbiology, Campus Box 8230, Washington University School of Medicine, 660 S. Euclid Ave, Campus Box 8230, Saint Louis, MO 63110; 314-747-2630.

Keywords: *Leishmania* RNA virus; LRV1; *Leishmania braziliensis*; endobiont viruses; virulence;

[e] Current address: New York Genome Center, 101 Avenue of the Americas, Office 627, New York, NY 10013.

AUTHOR CONTRIBUTIONS

Performed experiments: EAB, HZ, CR, L-FL, FMK, NSA, DMO, KLO, SMH

Designed experiments: EAB, HZ, CR, NF, SMB

Analyzed data: EAB, JS, CR, HZ, SMB

Wrote the manuscript: EAB, SMB

Abstract

Many *Leishmania (Viannia)* parasites harbor the double-stranded RNA virus *Leishmania RNA virus 1* (LRV1), which has been associated with increased disease severity in animal models and humans, and drug treatment failures in humans. Remarkably, LRV1 survives in the presence of an active RNAi pathway, which in many organisms controls RNA viruses. We found significant levels (0.4-2.5%) of small RNAs derived from LRV1 in both *L. braziliensis* and *L. guyanensis*, mapping across both strands and with properties consistent with Dicer-mediated cleavage of the dsRNA genome. LRV1 lacks *cis* or *trans*-acting RNAi inhibitory activities, suggesting that virus retention must be maintained by a balance between RNAi activity and LRV1 replication. To tilt this towards elimination, we targeted LRV1 using long-hairpin/stem-loop constructs similar to those effective against chromosomal genes. LRV1 was completely eliminated, at high efficiency, accompanied by a massive overproduction of LRV1-specific siRNAs, representing as much as 87% of the total. For both *L. braziliensis* and *L. guyanensis*, RNAi-derived LRV1-negative lines were no longer able to induce a Toll-like receptor 3-dependent hyper-inflammatory cytokine response in infected macrophages. This is the first demonstration of a role for LRV1 in *L. braziliensis* virulence *in vitro*, the *Leishmania* species responsible for the vast majority of mucocutaneous leishmaniasis cases. These findings establish the first targeted method for elimination of LRV1, and potentially of other *Leishmania* viruses, which will facilitate mechanistic dissection of the role of LRV1-mediated virulence. Moreover, our data establish a third paradigm for RNAi-viral relationships in evolution, one of balance rather than elimination.

Significance statement:

Leishmania parasites can be infected with *Leishmaniavirus* (LRV1), a double-stranded RNA virus whose presence in *L. guyanensis* parasites exacerbates disease severity in both mouse models and humans. Studies of the role of the virus on parasite biology and virulence are hampered by the dearth of isogenic lines bearing and lacking LRV, particularly in the clinically important species *L. braziliensis*. Here we describe a method to systematically generate LRV1-free *Leishmania* parasites using the parasite RNA interference (RNAi) pathway. The ability of transgene-driven RNAi to overcome the ability of LRV1 to withstand the endogenous RNAi attack suggests a new paradigm of virus-RNAi interaction, where RNAi and virus replication exist in balance to maintain persistent infection.

\body

Introduction

Leishmania is a genus of early-diverging protozoan parasites that cause leishmaniasis in many regions of the world, with an estimated 12 million symptomatic cases, at least 120 million asymptomatic cases, and nearly 1.7 billion at risk (1-5). The disease has three predominant clinical manifestations, ranging from the relatively mild cutaneous form to mucocutaneous disease, where parasites metastasize to and cause destruction of mucous membranes of the nose, mouth, and throat, and fatal visceral disease. Disease phenotypes segregate primarily with the infecting species; however, it is not fully understood which parasite factors affect severity and disease manifestations.

One recently identified parasite factor contributing to disease severity in *L. guyanensis* is the RNA virus *Leishmaniavirus* (6, 7). This virus is a member of the *Totiviridae* family, and consists of a single-segmented dsRNA genome that encodes only a capsid protein and an RNA-dependent RNA polymerase (RDRP) (8, 9). It is most frequently found (as LRV1) in New World parasite species in the subgenus *Viannia* such as *L. braziliensis (Lbr)* and *L. guyanensis (Lgy)*, which cause both cutaneous and mucocutaneous disease (6), but it has also been found sporadically in Old World subgenus *Leishmania* species (as LRV2) (10, 11). Like most totiviruses, LRV1 is neither shed nor infectious, and thus can be viewed as a long-term evolutionary endosymbiont whose activities on the mammalian host arise indirectly through the parasite, rather than by direct infection of the mammalian host by the virus (6). Previous work has shown that mice infected with LRV1-bearing strains of *Lgy* exhibit greater footpad swelling and higher parasitemia than mice infected with LRV1-negative *Lgy* (7). Similarly, macrophages infected *in vitro* with LRV1+ *Lgy* or LRV2+ *L.aethiopica* release higher levels of cytokines, phenotypes which were dependent on Toll-like receptor 3 (7, 10). The assignment of the LRV1-specificity of these phenotypes benefited greatly from the availability of a single isogenic LRV1-free line of *Lgy* (12).

Importantly, recent studies show that disease severity is increased in patients infected with LRV1+ *Lgy*, relative to LRV1-negative parasites (13).

In humans, *Lbr* is associated with cutaneous leishmaniasis, as well as the larger share of the more debilitating mucocutaneous leishmaniasis (MCL) (14, 15). While in some studies LRV1 was not correlated with MCL (16, 17), in others there was a strong association (6, 18, 19). Recent studies show that LRV1 in *Lbr* and *Lgy* clinical isolates correlates with drug treatment failure (16, 20). Thus, while other parasite or host factors may play a significant role in the development of MCL (21, 22), current data support a role for LRV1 in exacerbating the pathogenesis of human leishmaniasis caused by *Lbr and Lgy.* A similar role in pathogenicity has been proposed for the *Trichomonas vaginalis* totiviruses (23). In contrast, endobiont viruses in other systems more often impair the host or have no known effect on disease. Hypoviruses of *Cryphonectria parasitica* are associated with decreased virulence of their fungal host, while the L-A totivirus of *Saccharomyces cerevisiae* is not thought to affect pathogenicity, instead contributing to inter-microbial competition (24-27) .

Research into the role of LRV1 in *Lbr* disease is hampered by the fact that animal models are less well developed than for other *Leishmania* (28), and the absence of isogenic lines bearing or lacking LRV1. Since reverse genetic systems for *Totiviridae* do not exist and attempts to stably transfer LRV1 have proven unsuccessful (29), we asked whether RNA-interference (RNAi) could be used to generate LRV1-free isogenic isolates. Unlike Old World *Leishmania*, species of the *Viannia* subgenus, including *Lbr* and *Lgy*, retain an active endogenous RNAi pathway (30). The RNAi pathway converts double-stranded RNA into siRNAs, which trigger the degradation of an mRNA with complementary sequence (31). Importantly, the RNAi pathway acts as a defense against RNA viruses in plants and some animals, leading to great reductions or complete elimination (32, 33). Further, introduction of RNAi pathway proteins from *Saccharomyces castellii* into the naturally RNAi-null *S. cerevisiae* resulted in greatly decreased levels of persistently-infecting L-A totivirus (26). In mammals, siRNA-mediated RNAi activity

appears to play a smaller direct role in antiviral responses in adult mice (34, 35), although evidence of a direct response has been found in embryonic stem cells and young animals (36, 37).

Here we explore further the interactions of the RNAi pathway with LRV1 in both *Lbr* and *Lgy*, and show first that LRV1 is indeed seen by the endogenous RNAi pathway, as judged by the presence of significant levels of antiviral sRNAs. Thus and different than other systems, RNAi and viral replication appear to be balanced. However, by increased siRNA expression RNAi could be used to efficiently eliminate the virus. Importantly, these LRV1 negative transfectants recapitulate the *in vitro* macrophage cytokine release defect seen in naturally-occurring LRV1-negative lines, suggesting that the engineered LRV1-negative isogenic lines will be valuable in studying the role of LRV1-mediated biology and virulence.

Results

Naturally abundant siRNAs directed against LRV1 of L. braziliensis and L. guyanensis

Previous siRNA studies in *Leishmania* analyzed RNAs using a tagged Argonaute inserted into an *ago1*- knockout of *Lbr* M2903, which lacks LRV1 (9, 29, 38, 39). Because the lines bearing LRV1 studied here had not been similarly modified, we sequenced total small RNAs (sRNAs) as an alternative. *Lbr* siRNAs bear a 5'-P and 3'-OH, reflecting their origin through the action of cellular Dicer nucleases (39), and we used these properties to make siRNA-focused sRNA (<42 nt) libraries for next-generation sequencing (Table S1). For *Lgy* we chose the established LRV1+ *Lgy* M4147 strain (7), and three different *Lbr* shown to bear LRV1 by PCR and/or anti-dsRNA antibody tests (40).

For sRNAs from *Lbr* M2903 mapping to the *Lbr* reference genome, read length displayed a biphasic distribution, with a major peak centered around 23 nt (20-26 nt, 77.9% of total mapped reads) and a minor one around 33 nt (30-36nt, 9.4% of total mapped reads) (Fig. 1A, Table S1,S2). The 33 nt peak reads mapped primarily to structural RNA loci (62% of mapped reads; Table S2) similar to a sRNA class described in many eukaryotes including trypanosomes and *Leishmania* lacking the RNAi pathway

(41-44). In contrast, reads from the 23 nt peak showed properties similar to AGO1-bound siRNAs (39), including their size and the presence of 1-2 untemplated nucleotides at the 3' end in about 21% of the reads (Fig. 1A; Table S1). The 3' untemplated bases likely arise from the action of cellular terminal transferases, as *Leishmania* sp. lack the HEN1 methyltransferase that normally blocks their action (39). When both AGO1-bound siRNAs and the 23 nt sRNA peak reads were mapped to the *Lbr* genome their distributions were very similar, with the vast majority mapping to transposable elements (Figs. 1B, S2; Table S2) (39). We concluded that the 23 nt peak sRNAs (23 nt sRNAs) provides a reasonable proxy for siRNAs.

The properties of sRNAs from the LRV1-bearing *Lgy* M4147 and *Lbr* LEM2700, LEM2780 and LEM3874 mapping to the *Lgy* or *Lbr* reference genomes were similar to those of *Lbr* M2903, including the 23 and 33 nt sRNA peaks, genomic mappings, and the presence and level of 3' nt extensions in the 23nt sRNAs (Figs. 1, S1; Tables S1 & S2). Importantly, a substantial fraction of sRNA reads obtained from the LRV1+ *Lgy* and *Lbr* lines mapped to the LRV1 genomes, ranging from 0.4-2.5% of the 23nt mapped reads (Fig. 1B, Table S1). Unlike those aligned to the nuclear genome, LRV1-mapped reads showed a single size distribution centered around 23 nt (Fig. 1A), with about 20% again showing short 3' extensions (Table S1), typical of *Lbr* siRNAs and 23 nt sRNAs (39). LRV1-mapping 23 nt sRNAs showed no consistent strand- or region-specific biases in all four strains (Fig. S2), suggesting that they likely originated from the action of DICERs on the viral dsRNA genome.

We previously showed that LRV1 does not encode a *trans*-acting inhibitor of RNAi activity (30), and the presence of high levels of LRV1-directed sRNAs similarly suggests that it does not encode a strong *cis*-acting inhibitor. Importantly, the levels of 23 nt sRNAs mapping to LRV1s were in the same range as siRNAs mapping to an efficiently silenced Luciferase reporter (0.4–2.5% vs. 0.8% targeted by long hairpin/stem loop transgene) (30, 39). Thus, LRV1 is able to persist in the face of a significant RNAi response, as judged by 23 nt sRNA levels.

LRV1 can be efficiently targeted by transgenic RNAi

These data are consistent with a model where RNAi activity and LRV1 replication has achieved a 'balance' between viral synthesis and degradation, which might be shifted by increasing or decreasing RNAi activity. With an eye towards virus elimination, we focused on increasing LRV1-targeting siRNA levels through the use of transgenic RNAi methods developed previously (30), in which long hairpin RNA is expressed at high levels from a stem-loop (StL) construct containing LRV1 sequences integrated into the ribosomal RNA locus (Fig. 2A). We targeted regions of LRV1 from the capsid or RDRP ORFs (*Lgy* M4147, *Lbr* LEM2700 and LEM2780), or a region that spanned them (*Lbr* LEM3874), ranging in length from 794 to 1,143 bp (Fig. 2B & Table S3); since the two viral genes reside within the same RNA segment, targeting either should lead to degradation of the entire LRV1 RNA. Since LRV1 sequences diverge substantially between parasite strains (69-90% nt identity), 'stems' specific for each species/strain were used. To assess non-specific effects, we integrated an StL construct for an AT-rich GFP (GFP65 StL), which efficiently silences expression of GFP65 (30). The untransfected parental lines served as LRV1+ controls, and *Lbr* M2903 or *Lgy* M4147/HYG (12) served as LRV1-negative controls.

To screen for loss of LRV1, StL transfectants were analyzed by flow cytometry of fixed, permeabilized cells using an antibody raised against the *Lgy* M4147 LRV1 capsid (45), which cross reacts with *Lbr* LRV1. For both *Lgy* M4147 (Fig. 3, top) and *Lbr* LEM2780 (Fig. 3, bottom), there was a clear separation in capsid staining between the LRV1-positive (red) and LRV1-negative controls (green). While control GFP65 StL lines (purple) had capsid protein levels similar to WT, capsid protein was undetectable in LRV1-targeted StL lines (Fig. 3, light & dark blue), indistinguishable from the LRV1-negative control. This was observed whether the capsid or RDRP was targeted (Fig. 3). Similar results were obtained with LRV1 StL transfectants from *Lbr* LEM2700 and *Lbr* LEM3874. In support of the flow cytometry data, western blot analysis with an anti-capsid antibody showed high LRV1 levels in the *Lgy* parental line and GFP65 StL transfectants, while capsid protein was undetectable in the capsid StL transfectants (Fig. S3).

StL constructs result in high levels of siRNAs mapping to the LRV1 stem

Despite the insensitivity of LRV1 to 'natural' levels of RNAi, as judged by the abundance of 23nt sRNAs, introduction of StL constructs targeting LRV1 resulted in great reduction in LRV1 levels. To understand the basis for this, we analyzed 23 nt sRNA peak reads mapping to the nuclear and LRV1 genomes, for one LRV1 StL transfectant of each species (Fig. 4). Remarkably, the percentage of total 23 nt sRNAs mapping to LRV1 had increased greatly from that seen in the WT parent, from 2.5% to 86.7% for *Lgy* and from 1.8% to 73.0% for *Lbr* LEM3874 (Figs. 4A, S4). Concomitantly, the percentages of 23 nt sRNAs mapping to the nuclear genome was proportionately reduced, with some variability amongst loci and/or lines (for example, rRNA reads were unchanged in both species, while tRNA reads decreased in *Lgy*; Figs. 4A, S1A). While we did not measure the absolute levels of sRNAs, previous studies show these are tightly controlled by the level of Argonaute 1 and thus are unlikely to differ significantly (39). Essentially all LRV1-mapping sRNAs in LRV1 StL lines now mapped only to the RNAi-targeted 'stem' region (Fig. 4B, dark grey), as expected since LRV1 had been eliminated (below). This also argues against the occurrence of 'transitive' siRNA formation (46, 47).

The levels of LRV1 23 nt sRNAs (76-87%) in LRV1 StL-transfectants were much greater than seen with siRNAs mapping to the LUC ORF/stem targeted using the same StL transfection construct (0.8%) (39). To rule out the possibility that this arose from reliance on 23nt sRNAs, we analyzed these from a line bearing the LUC StL RNAi reporter used in the siRNA studies (IR2-LUCStL(b)-LUC(a)). For this, 1.14% of the 23nt sRNA peak reads mapped to the LUC ORF/stem, suggesting that use of 23nt sRNAs vs siRNAs did not significantly impact quantitation. To assess the target-specific effects, we compared these results with those quantitating 23 nt peak sRNAs after RNAi StL targeting of a panel of 10 chromosomal genes. For this group, 1.5-34% of 23 nt sRNAs mapped to the RNAi-targeted gene, compared to less than 0.02% basally. Thus, the StL-bearing IR vectors generate a high but variable level of sRNAs for all genes tested, with the LUC reporter being at the low end and LRV1 at the high end. This may reflect the fact that while

the LRV1 target is typically eliminated by RNAi (Fig. 3 and below), chromosomal RNAi targets continuously transcribe mRNAs. In other organisms, studies have shown that the presence of a cognate target facilitates the turnover of sRNAs; thus, the absence of LRV1 target may lead to higher levels of siRNAs (48, 49). Future studies may address the factors contributing to the differences in sRNA levels amongst genes and to the very high steady-state levels of LRV1-directed 23 nt sRNAs seen here.

Complete virus elimination following RNAi of LRV1

RNAi-mediated LRV1 knockdown would be most useful as a tool if it resulted in a complete elimination of LRV1. To achieve a sensitivity beyond that of flow cytometry (~20 fold) or western blotting (~100 fold), we validated a sensitive quantitative RT-PCR assay (qRT-PCR) for LRV1, using strain- and LRV1-specific primers to amplify a region located outside the 'stem' regions (Table S4; Fig. 2B). Since the melting temperatures of PCR amplicons are sequence- and length-dependent, comparison of dissociation (melt) curves facilitated discrimination between specific and non-specific amplification.

Because LRV1 copy number was estimated to be ~100/cell (50), a cutoff for classification as LRV1-negative was set at 10^4-fold below WT. Analysis of *Lbr* qPCR data by the $\Delta\Delta C_t$ method (51) showed that most LRV1 StL transfectants had LRV1 RNA levels more than 10^5-fold lower than WT (Figs. 5A, S5A,B). Raw C_t values for LRV1 StL lines with LRV1-specific primers were indistinguishable from mock cDNA preparations, and ΔC_t values were indistinguishable from those of negative controls. Melt curves show that products seen at C_t arose from non-specific amplification (Figs. 5A, S5A,B; white bars). As expected for control GFP65 StL lines, LRV1 RNA levels were similar to those in WT (Figs. 5A, S5A,B; black bars).

Similar results were obtained with RNAi of LRV1 in *Lgy* M4147, with most transfectants showing reductions below the 10^4-fold cutoff (Fig. 5B). However, low levels of LRV1 remained in two lines where the RDRP was targeted, approximately 300- to 500-fold less than the parent line (Fig. 5B, black bars); here melt curve analysis suggested these products were LRV1-specific. Alternate primers targeting other

regions across the virus gave similar results, suggesting the presence of intact LRV1. We hypothesized that this was due to heterogeneity in viral load, with most but not all cells lacking LRV1. In support of this, we generated and showed that all clonal lines arising from one of the "weakly positive" lines were negative for LRV1 by flow cytometry and satisfied the 10^4-fold cutoff by qPCR (Fig. S5C). The occasionally incomplete LRV1 elimination is consistent with our prior observation that RNAi was somewhat less efficient in *Lgy* than in *Lbr* (30). Nonetheless, even for "weakly positive" *Lgy* transfectants, RNAi was sufficiently efficient for the ready isolation of LRV1-negative lines (Fig. 3, top; 5B; S3).

LRV1 knockdowns induce less cytokine production in in vitro *macrophage infection assays*

Previous reports showed that LRV1+ *Lgy* stimulated the TLR3-dependent release of higher levels of cytokines from bone marrow-derived macrophages (BMDMs) than LRV1-negative strains (7). The availability of defined RNAi-derived LRV1-negative lines now allowed tests of this in *Lbr* for the first time as well as confirmation of prior results obtained with a single isogenic LRV1- *Lgy*. Briefly, BMDMs were infected *in vitro* with LRV1 StL and GFP65 StL *Lbr* and *Lgy* transfectants, as well as positive and negative control lines, and the levels of two cytokines known to be induced by LRV1 (TNF-α and IL-6) (7, 10) were measured.

Capsid StL and RDRP StL LRV1-negative lines of both *Lbr* and *Lgy* induced significantly lower levels of cytokine production than did the LRV1-positive lines (both parental and GFP65 STL) (Fig. 6, Fig. S5). Additionally, when macrophages from TLR3-deficient mice were infected with *Lbr* LEM2700, the LRV1-positive parasites no longer elicited higher levels of cytokine release (Fig. S5). Of note, all *Lgy* LRV1 StL lines induced background levels of cytokine release, including the two lines that retained low levels of LRV1 (Fig. 5B & 6B, Fig. S5), consistent with the observation that high levels of LRV1 were necessary for cytokine stimulation (7, 10).

Discussion

In this study we have characterized the endogenous RNAi response in *Leishmania* bearing the dsRNA virus LRV1, and used these insights to generate virus-negative lines that facilitate the study of the role of LRV1 in parasite biology and host-parasite interactions.

Leishmania LRV1 and the endogenous RNAi pathway

We identified two populations of sRNA in *Lbr* and *Lgy*. The less abundant 33 nt sRNAs mapped primarily to genes encoding structural RNAs (Table S2), as seen in other organisms including trypanosomatids (41-44). In contrast, the more abundant 23 nt sRNA fraction exhibited properties similar to authentic, AGO1-bound *Lbr* siRNAs (39), including size, the presence of 3' untemplated bases at the same frequency (~20%), and mapping primarily to transposable elements and repetitive sequences (Fig 1; Tables S1 & S2). Only 23 nt sRNA reads mapped to the LRV1 dsRNA genome (Fig. 1A), and these also bore 3' nucleotide extensions at the same frequency, again consistent with an origin via the RNAi pathway (Table S1). Importantly, the levels of 23 nt sRNAs mapping to LRV1 constituted a substantial fraction of total aligned 23nt sRNAs (Fig 1B, Table S1), comparable to those targeting an efficiently-silenced LUC reporter gene (30, 39). Thus, LRV1 can persist in the face of RNAi pressure that gives rise to sRNA levels comparable to that which efficiently silences a chromosomal target gene.

In other organisms, sRNA/siRNA levels provide a gauge of RNAi pathway recognition and targeting of viruses: when RNAi controls virus replication, as in plants, fungi, and insects (26, 32, 33), high levels of siRNAs accompany viral infections, leading to eradication of the virus. In mammals, quantitatively fewer siRNAs are present, which do not effectively control virus levels, at least in adult somatic tissues (34, 36, 37). In contrast, high levels of siRNA-like 23 nt sRNAs in *Leishmania* suggest an attack on LRV1 by the RNAi pathway, but the virus persists. While many viruses encode *trans*-acting RNAi suppressors mediating their survival (52), this seems unlikely for LRV1. There is no obvious coding potential for this in the compact LRV1 genome, our studies here suggest there is no strong *cis*-acting

inhibitory activity, and we showed previously that a luciferase reporter was equally silenced in the LRV1+ and LRV1-negative *Lgy* studied here (30). This suggests a third model where LRV1 is targeted strongly by the RNAi pathway, but the RNAi-mediated degradation is 'balanced' by virus replication or other factors. We are currently working to identify which component(s) of the RNAi machinery mediate this balance. While the slicer activity of Argonaute is perhaps the most likely agent, previous studies examining the role of RNAi in control of viruses frequently raise the possibility of Dicer-mediated control as well (53-55). It is likely that the sequestration of the LRV1 dsRNA genome within the capsid may also contribute by limiting the exposure of the LRV1 dsRNA to the RNAi machinery and other degradative pathways. In yeast, *SKI* genes act to prevent deleterious effects of L-A viruses towards its fungal host through alterations in mRNA degradation and/or surveillance (27), and homologous genes for several of these are evident in the *Leishmania* genome.

In other organisms, persistent viruses can also be maintained in the face of an active RNAi pathway, but at considerably reduced levels (26, 56). Over evolutionary time, this strong pressure likely accounts for the inverse relationship in fungi between virus levels and the activity and/or presence of the RNAi pathway, especially when associated with a selective advantage for viral retention, as seen with the yeast killer factors which are dependent on the L-A virus (26, 57). Similarly, in *Leishmania* we had originally proposed that RNAi pressure would be sufficiently strong as to in some cases provide a driving force for loss of RNAi, in order to maintain LRV1-dependent increases in pathogenicity (30). Given the greater ability of LRV1 to survive in the presence of an active RNAi pathway, our data suggest that the magnitude of this effect may be considerably less than envisioned. However, even small pressure could prove a significant force towards down-regulating pathways impacting on LRV1 levels during evolution.

RNAi as a tool for generating LRV1-negative lines for biology

Following the predictions of the 'balance' hypothesis, we aimed to increase activity against LRV1 through the increased synthesis of siRNAs targeting LRV1. This proved quite successful; the fraction of 23 nt sRNAs targeting LRV1 rose dramatically in lines expressing StL constructs targeting LRV1 (Figs. 1B & 4A). Correspondingly, the fraction of 23 nt sRNAs mapping to the *Leishmania* genome dropped proportionately, most of which again mapped to TEs and repeats (Fig. 4A). Importantly, LRV1 levels were dramatically reduced for all LRV1 StL transfectants, and in most cases the virus eliminated, as judged by protein and RNA methods (Figs. 3, 5, S3, S5). Targeting of either the capsid or RDRP gene eliminated LRV1, as was expected given that both are encoded by the same RNA (Fig. 2A). Only in *Lgy* were some transfectants found that retained low levels of LRV1, which could reflect less RNAi activity in this species, as was seen with reporter genes (30). However, most transfectants had completely lost LRV1.

Viral infection has been reported for *Giardiavirus* (58), and stable viral transfer for several fungal Totiviruses (59). However*, de novo* infection and stable viral transfer have been unsuccessful with *Lgy* (29), and reverse genetic systems have yet to be reported for any Totivirus. Therefore, the ability to reproducibly mediate viral cure by RNAi is of great value for biological studies of LRV1. Previous work used an LRV1-negative *Lgy* which was obtained following transfection with an episomal *Leishmania* vector expressing resistance to hygromycin B, followed by a long period of growth under selection (12); however, this method seems to have been successful only once. Neither have we succeeded with several 'stress-related' treatments that have proven effective in curing mycoviruses, such as yeast L-A (60). Our studies establish RNAi as a viable strategy for cure of LRV1 and perhaps other viruses in RNAi-competent *Leishmania* species.

LRV1+ but not LRV1-negative *Lgy* induce a 'hyperinflammatory' cytokine response in infections of BMDMs *in vitro*, which is TLR3-dependent (6, 7). Infectivity tests of mouse BMDMs *in vitro* showed that RNAi-generated LRV1-negative *Lgy* lines likewise failed to induce a substantial cytokine response, as shown for two cytokines (TNF-α and IL-6) known to be diagnostic for an LRV1-driven innate immune

response. Interestingly, this occurred with RNAi-derived lines where LRV1 loss was substantial but incomplete (RDRP StL c3 & 4; 500- and 300-fold below parental levels, respectively; Fig 5B, 6B, S7), consistent with data from natural *Lgy* showing low LRV1 levels (7). Thus, a partial reduction in LRV1 levels is sufficient to ameliorate LRV1-dependent virulence, which may facilitate future efforts targeting LRV1 in human disease. Importantly, the continued presence of the integrated StL constructs appeared to have no 'off target' effect in the BMDM infections, despite the high levels of transgene-derived 23 nt sRNAs present in these lines; the LRV1 StL "cured" lines induced the release of cytokines at a level similar to that of StL-negative, LRV1-negative controls (Fig. 4), and control GFP65 StL lines that maintained LRV1 induced the release of cytokines at a level similar to the StL-negative, LRV1+ parent (Fig. 3, 5, 6). Future studies will assess whether this also pertains to other cell types or host infections.

LRV1-dependent virulence in Leishmania braziliensis

Previous studies of LRV1-dependent virulence focused primarily on *Lgy*; however, in humans, *Lbr* is associated with the larger share of MCL (14, 15). Our studies extend the generality of LRV1-dependent virulence to *Lbr,* as LRV1+ *Lbr* likewise induce strong TLR3-dependent cytokine responses. These findings are especially important in light of published work on the association of LRV1 with MCL, with mixed results depending on the geographic region and methods used (6, 16-19). Our data show that in *in vitro* infections, LRV1 contributes strongly to the pro-inflammatory phenotype associated with elevated pathogenicity, as seen in *Lgy*. This suggests that in human infections it may be informative to seek for correlations between LRV1 and the severity of CL in *Lbr* infections in future studies. Indeed, recent studies show that LRV1 in *Lbr* clinical isolates correlates with drug treatment failure (16), as was also seen in *Lgy* (20). Thus, while other parasite or host factors may play a significant role in the development of MCL (21, 22), current data now bolstered by our studies of isogenic LRV1+/negative lines support a role for LRV1 in severity of human leishmaniasis caused by *Lbr.*

Methods

Parasites and in vitro culture

Lbr LEM2700 (MHOM/BO/90/AN), LEM2780 (MHOM/BO/90/CS) and LEM3874 (MHOM/BO/99/IMT252 n°3) were from Patrick Bastien (Université de Montpellier), *Lbr* M2903 (MHOM/BR/75/M2903) was from Diane McMahon Pratt (Yale School of Public Health), and *Lgy* M4147 (MHOM/BR/78/M4147) and its derivative *Lgy* M4147/HYG was from Jean Patterson (Southwest Foundation for Biomedical Research, San Antonio, Texas). Prior to introduction of StL constructs, parasites were transfected with the linear SSU-targeting SwaI fragment from B6367 pIR2SAT-LUC(B) (30), and clonal lines were derived, validated, and used. The luciferase-expressing clone of *Lbr* LEM2780 contained only LRV1-*Lbr*LEM2780(b). Parasites were grown in fresh Schneider's Insect Medium supplemented with 10% heat-inactivated fetal bovine serum, 100 µM adenine, 10 µg/mL hemin, 2 µg/mL biopterin, 2 mM L-glutamine, 500 units/ml penicillin and 50 ug/mL streptomycin, and selective drugs as indicated below.

RNAi Stem-loop Constructs

Regions of interest from LRV1 were screened using the RNAit target selection tool to ensure that there was no homologous sequence in the parasite genome (61), amplified from cDNA by PCR using KlenTaq-LA polymerase, and cloned into the pCR8/GW/TOPO cloning vector (Thermo Fisher Scientific, Waltham, Massachusetts) using the protocol recommended by the manufacturer and a 20 min ligation. The 'stem' segments and PCR primer sequences can be found in Table S3. The 'stems' were transferred from the pCR8/GW/TOPO donor vector to the pIR2HYG-GW(A) (B6365) destination vector (which contains sequence from the parasite rRNA locus to enable integration into the genome and inverted LR recombinase sites for the generation of inverted repeat through Gateway© technology) using LR Clonase II (Thermo Fisher) in an overnight reaction at room temperature. Reactions were terminated by incubating with proteinase K for 1 hour at 37°C. Constructs were verified by restriction digest.

Transfections

Stable transfections were performed as previously described (30, 62). Clonal lines were obtained by plating on semisolid media with 50 μg/mL hygromycin B. After colonies formed, cells were grown to stationary phase in 1 mL media and passaged thereafter in 10 mL media with 30 μg/mL hygromycin B.

RNA preparation and quantitative real-time PCR (qPCR)

Total RNA was prepared from log-phase cells dissolved in Trizol reagent (Thermo Fisher) at 3 x 10^8 cells/mL using the Direct-zol kit (Zymo Research, Irvine, California) and eluted in 50 μL of nuclease-free water. The RNA was DNAseI-treated (Thermo Fisher) in a 200 μL reaction using the provided buffer and 20 Units of enzyme for 1 hour at 37 °C, purified using the RNA Clean & Concentrator - 25 kit (Zymo Research), and eluted in 50 μL of nuclease-free water. Reverse transcription was performed using the Superscript III first-strand synthesis kit (Thermo Fisher) according to the manufacturer instructions in a 20 μL reaction containing 0.25 ug purified RNA. Control reactions contained the same amount of RNA but lacked reverse transcriptase enzyme. For qRT-PCR, primers were designed to amplify ~100 bp regions of the LRV1 genome that lie outside the stem regions (Table S4). qPCR reactions were performed with cDNA templates in 20 μL total reaction volume using the Power SYBR Green Master Mix (Thermo Fisher), 5 μL of ten-fold diluted cDNA, and final primer concentrations of 0.2 μM. Reactions were run on the ABI PRISM 7000 Sequence Detection System (Applied Biosystems, Thermo Fisher). PCR amplification conditions were as follows: 50 °C for 2 min and 95 °C for 10 sec followed by 40 cycles of 95 °C for 15 sec and 60 °C for 1 min. PCR products were confirmed to be specific by melt curve analysis. All experiments were performed in triplicate. Amplification of KMP-11 was used as an internal control to normalize parallel reactions.

Small RNA (sRNA) sequencing

sRNA libraries were generated from total RNA as described (39); briefly, a primer (5'-rApppATCTCGTATGCCGTCTTCTGCTTG/ddC for all samples except *Lgy* M4147, which used primer rApppTGGAATTCTCGGGTGCCAAGG/ddC) was ligated first to the 3' end using truncated mutant T4 RNA Ligase (New England Biolabs), and then a second riboprimer (5'-GUUCAGAGUUCUACAGUCCGACGAUC) to the 5' end with T4 RNA Ligase**.** cDNA was generated using reverse transcriptase and primer 5'-CAAGCAGAAGACGGCATACGA, and then PCR was performed with this in conjunction with primer 5'-AATGATACGGCGACCACCGACAGGTTCAGAGTTCTACAGTCCGA. Products corresponding to inserts of 10-50 nt were purified, and taken for sequencing with Illumina HiSeq2500 technology. Sequences have been deposited in the NCBI Short Read Archive (accession SRP082553).

Bioinformatic analysis of sRNAs

The 5' and 3' adapter sequences were removed from the sRNA reads, those less than 15 nt removed, and the trimmed reads were mapped to homologous LRV1 or *Leishmania* genomes (*Lbr* M2904 (63) or a draft *Lgy* M4147 genome (Bioproject PRJEB82; accession CALQ01000001 – CALQ01004013)) using Novoalign software http://www.novocraft.com; parameters were set as -F ILMFQ; -H; -g 40; -x 6; -R 5; -r; and -e 1000). A random strategy was employed to align reads mapping to multiple regions and hard clipping of low coverage bases at 3' end was performed. sRNA abundance was assessed directly, or after 'collapsing' to remove duplicate reads using algorithms within the fastx toolkit (http://hannonlab.cshl.edu/fastx_toolkit/index.html). To annotate transposable or repeated elements, we used RepeatMasker (http://www.repeatmasker.org) to identify known elements and/or BLAST to identify regions corresponding to *Leishmania* specific elements (SLACS, TAS, and TATE (63)) . The annotations were collected in .bed file format for further use. Coverage was calculated by counting the number of reads that align to each strand of the LRV1 genome.

LRV1 sequences

From the sRNA sequences we assembled whole or partial LRV1 contigs, which were confirmed and completed by PCR amplification and sequencing. The sequences for LRV1-*Lbr*LEM2700, LRV1-*Lbr*LEM2780(a) and (b), LRV1-LbrLEM3874, and a revision of the LRV1-LgyM4147 (formerly LRV1-4; (64)) genome sequences were deposited in GenBank (accession numbers KX808483-KX808487).

LRV1 capsid flow cytometry.

The development and optimization of this protocol will be described elsewhere (F.M. Kuhlmann et al. in preparation). Briefly, 1 x 10^7 cells were fixed at room temperature (RT) using 2% paraformaldehyde (Thermo Fisher) in PBS for 2 min, and then then incubated in blocking/permeabilization buffer (BPB) (10% normal goat serum(Vector Laboratories) and 0.2% Triton X-100 in PBS) for 30 min, at RT. Anti-*Lgy* LRV1 capsid antibody (45) was added (1:20,000 dilution) and incubated at RT for 1 hr. After two washes with PBS, cells were resuspended in 200 µl BPB with Alexa488-labeled goat-anti-rabbit antibody (Thermo Fisher) (1:2,000 dilution) and incubated 1 hr at RT. After two additional washes with PBS, cells were subjected to flow cytometry and the data analyzed using CellQuest© software (BD Bioscience).

Western blot, macrophage infections and cytokine assays.

After an initial wash with PBS, 5x10^7 parasites were resuspended in 100 µL of 1x PBS. 1x10^7 cells (20 µL) were lysed with 7 µL of 4x Laemmli's gel sample buffer. After heating for 5 min at 95 °C, cell lysates were loaded and separated on a 10% polyacrylamide denaturing gel, transferred to a nitrocellulose membrane and visualized by Ponceau Red staining. The membrane was blocked for 1h in 5% powdered milk diluted in TBS + 0.05% Tween20, incubated overnight at 4 °C with the g018d53 anti-capsid polyclonal antibody (1:5000 in 1% milk TBS-Tween20), washed 4x 15 min at RT, incubated for 1h with an anti-rabbit IgG antibody coupled to peroxidase (Promega) (1:2500 in 1% milk TBS-Tween20), washed again 4x and finally revealed by ECL chemiluminescence (Amersham). Infections of BL6 mouse BMDM and cytokine assays were performed as previously described (7, 10).

Statement identifying institutional and/or licensing committee approving animal experiments.

Animal handling and experimental procedures were undertaken with strict adherence to ethical guidelines relevant in both host countries. These are set out by the SFVO and under inspection by the Department of Security and Environment of the State of Vaud, Switzerland. Experiments were carried out in strict accordance with the recommendations in the Guide for the Care and Use of Laboratory Animals of the United States National Institutes of Health. Animal studies were approved by the Animal Studies Committee at Washington University (protocol #20090086) in accordance with the Office of Laboratory Animal Welfare's guidelines and the Association for Assessment and Accreditation of Laboratory Animal Care International.

Acknowledgments

This work was supported in part by NIGMS Cell and Molecular Biology Training Grant GM: 007067 and the Monsanto Excellence Fund for Graduate Fellowships (EAB), NIH grants RO1AI029646 and R56AI099364 (SMB), grants FNRS N° 3100A0-116665/1 and IZ70Z0-131421 (NF), and the Division of Infectious Diseases (FMK). We thank D.E. Dobson for comments on this manuscript, Florence Prevel for excellent technical support, Jean Patterson (Southwest Foundation for Biomedical Research, San Antonio, Texas) for providing *Lgy* M4147 and anti-capsid antisera, P. Bastien (U. Montpellier, Montpellier FR) for *Lbr* strains, and S P. Calderon-Copete for use of draft *Lgy* genome. Next-generation sequencing was performed at the Washington University School of Medicine, Dept. of Genetics Genome Technology Access Center (partially supported by grants NCI Cancer Center Support P30 CA91842 and NCRR ICTS/CTSA UL1 TR000448).

References.

1. Alvar J*, et al.* (2012) Leishmaniasis worldwide and global estimates of its incidence. *PLoS One* 7(5):e35671.
2. Banuls AL*, et al.* (2011) Clinical pleiomorphism in human leishmaniases, with special mention of asymptomatic infection. *Clin Microbiol Infect* 17(10):1451-1461.
3. Singh OP, Hasker E, Sacks D, Boelaert M, & Sundar S (2014) Asymptomatic *Leishmania* infection: a new challenge for *Leishmania* control. *Clin Infect Dis* 58(10):1424-1429.
4. Pigott DM*, et al.* (2014) Global distribution maps of the leishmaniases. *Elife* 3.
5. WHO (2010) Control of the Leishmaniases: WHO Expert Committee on the Control of Leishmaniases. *World Health Organization Technical Reports* 949:1-186.
6. Hartley MA, Drexler S, Ronet C, Beverley SM, & Fasel N (2014) The immunological, environmental, and phylogenetic perpetrators of metastatic leishmaniasis. *Trends Parasitol* 30(8):412-422.
7. Ives A*, et al.* (2011) *Leishmania* RNA virus controls the severity of mucocutaneous leishmaniasis. *Science* 331(775).
8. Widmer G, Comeau aM, Furlong DB, Wirth DF, & Patterson JL (1989) Characterization of a RNA virus from the parasite *Leishmania*. *Proc Natl Acad Sci USA* 86(15):5979-5982.
9. Stuart KD, Weeks R, Guilbride L, & Myler PJ (1992) Molecular organization of *Leishmania* RNA virus 1. *Proc Natl Acad Sci USA* 89(18):8596-8600.
10. Zangger H*, et al.* (2014) *Leishmania aethiopica* field isolates bearing an endosymbiontic dsRNA virus induce pro-inflammatory cytokine response. *PLoS neglected tropical diseases* 8(4):e2836-e2836.
11. Scheffter SM, Ro YT, Chung IK, & Patterson JL (1995) The complete sequence of *Leishmania* RNA virus LRV2-1, a virus of an Old World parasite strain. *Virology* 212:84-90.
12. Ro YT, Scheffter SM, & Patterson JL (1997) Hygromycin B resistance mediates elimination of *Leishmania* virus from persistently infected parasites. *Journal of Virology* 71(12):8991-8998.
13. Hartley MA*, et al.* (2016) *Leishmaniavirus*-Dependent Metastatic 1 Leishmaniasis Is Prevented by Blocking IL-17A. *PLos Pathogens* in press.
14. Guerra JA*, et al.* (2011) Mucosal Leishmaniasis caused by *Leishmania (Viannia) braziliensis* and *Leishmania (Viannia) guyanensis* in the Brazilian Amazon. *PLoS Negl Trop Dis* 5(3):e980.
15. Goto H & Lindoso JAL (2010) Current diagnosis and treatment of cutaneous and mucocutaneous leishmaniasis. *Expert Review of Anti-infective Therapy* 8(4):419-433.

16. Adaui V*, et al.* (2016) Association of the Endobiont Double-Stranded RNA Virus LRV1 With Treatment Failure for Human Leishmaniasis Caused by *Leishmania braziliensis* in Peru and Bolivia. *J Infect Dis* 213(1):112-121.
17. Pereira Lde O*, et al.* (2013) Severity of tegumentary leishmaniasis is not exclusively associated with *Leishmania* RNA virus 1 infection in Brazil. *Mem Inst Oswaldo Cruz* 108(5):665-667.
18. Cantanhede LM*, et al.* (2015) Further Evidence of an Association between the Presence of *Leishmania* RNA Virus 1 and the Mucosal Manifestations in Tegumentary Leishmaniasis Patients. *PLoS Negl Trop Dis* 9(9):e0004079.
19. Ito MM*, et al.* (2015) Correlation between presence of *Leishmania* RNA virus 1 and clinical characteristics of nasal mucosal leishmaniosis. *Braz J Otorhinolaryngol* 81(5):533-540.
20. Bourreau E*, et al.* (2016) Presence of *Leishmania* RNA Virus 1 in *Leishmania guyanensis* Increases the Risk of First-Line Treatment Failure and Symptomatic Relapse. *J Infect Dis* 213(1):105-111.
21. Castellucci LC*, et al.* (2014) Host genetic factors in American cutaneous leishmaniasis: a critical appraisal of studies conducted in an endemic area of Brazil. *Mem Inst Oswaldo Cruz* 109:279-288.
22. Schriefer A, Wilson ME, & Carvalho EM (2008) Recent developments leading toward a paradigm switch in the diagnostic and therapeutic approach to human leishmaniasis. *Curr Opin Infect Dis* 21(5):483-488.
23. Fichorova RN*, et al.* (2013) Endobiont viruses sensed by the human host - beyond conventional antiparasitic therapy. *PLoS One* 7(11):e48418.
24. Dawe AL & Nuss DL (2001) Hypoviruses and chestnut blight: exploiting viruses to understand and modulate fungal pathogenesis. *Annu Rev Genet* 35:1-29.
25. Dawe AL & Nuss DL (2013) Hypovirus molecular biology: from Koch's postulates to host self-recognition genes that restrict virus transmission. *Adv Virus Res* 86:109-147.
26. Drinnenberg Ia, Fink GR, & Bartel DP (2011) Compatibility with killer explains the rise of RNAi-deficient fungi. *Science* 333(6049):1592-1592.
27. Wickner RB, Fujimura T, & Esteban R (2013) Viruses and prions of *Saccharomyces cerevisiae*. *Adv Virus Res* 86:1-36.
28. Mears ER, Modabber F, Don R, & Johnson GE (2015) A Review: The Current *In Vivo* Models for the Discovery and Utility of New Anti-leishmanial Drugs Targeting Cutaneous Leishmaniasis. *PLoS Negl Trop Dis* 9(9):e0003889.

29. Armstrong TC, Keenan MC, Widmer G, & Patterson JL (1993) Successful transient introduction of *Leishmania* RNA virus into a virally infected and an uninfected strain of *Leishmania*. *Proc Natl Acad Sci USA* 90(5):1736-1740.
30. Lye L-F*, et al.* (2010) Retention and loss of RNA interference pathways in trypanosomatid protozoans. *PLoS Pathogens* 6(10):e1001161-e1001161.
31. Wilson RC & Doudna JA (2013) Molecular mechanisms of RNA interference. *Annu Rev Biophys* 42:217-239.
32. Hu Q, Niu Y, Zhang K, Liu Y, & Zhou X (2011) Virus-derived transgenes expressing hairpin RNA give immunity to Tobacco mosaic virus and Cucumber mosaic virus. *Virology Journal* 8(1):41-41.
33. Tompkins SM, Lo C-Y, Tumpey TM, & Epstein SL (2004) Protection against lethal influenza virus challenge by RNA interference in vivo. *Proc Natl Acad Sci USA* 101(23):8682-8686.
34. Cullen BR, Cherry S, & tenOever BR (2013) Is RNA interference a physiologically relevant innate antiviral immune response in mammals? *Cell Host Microbe* 14(4):374-378.
35. Umbach JL & Cullen BR (2009) The role of RNAi and microRNAs in animal virus replication and antiviral immunity. *Genes Dev* 23(10):1151-1164.
36. Li Y, Lu J, Han Y, Fan X, & Ding SW (2013) RNA interference functions as an antiviral immunity mechanism in mammals. *Science* 342(6155):231-234.
37. Maillard PV*, et al.* (2013) Antiviral RNA interference in mammalian cells. *Science* 342(6155):235-238.
38. Tarr PI*, et al.* (1988) LR1: a candidate RNA virus of *Leishmania*. *Proc Natl Acad Sci USA* 85(24):9572-9575.
39. Atayde VD*, et al.* (2013) The structure and repertoire of small interfering RNAs in *Leishmania* (*Viannia*) *braziliensis* reveal diversification in the trypanosomatid RNAi pathway. *Molecular Microbiology* 87(3):580-593.
40. Zangger H*, et al.* (2013) Detection of *Leishmania* RNA virus in *Leishmania* parasites. *PLoS Neglected Tropical Diseases* 7(1):e2006-e2006.
41. Thompson DM & Parker R (2009) Stressing out over tRNA cleavage. *Cell* 138(2):215-219.
42. Garcia-Silva MR*, et al.* (2010) A population of tRNA-derived small RNAs is actively produced in *Trypanosoma cruzi* and recruited to specific cytoplasmic granules. *Mol Biochem Parasitol* 171(2):64-73.
43. Franzen O*, et al.* (2011) The short non-coding transcriptome of the protozoan parasite *Trypanosoma cruzi*. *PLoS Negl Trop Dis* 5(8):e1283.

44. Lambertz U*, et al.* (2015) Small RNAs derived from tRNAs and rRNAs are highly enriched in exosomes from both old and new world Leishmania providing evidence for conserved exosomal RNA Packaging. *BMC Genomics* 16:151.
45. Cadd TL, Keenan MC, & Patterson JL (1993) Detection of *Leishmania* RNA virus 1 proteins. *Journal of Virology* 67(9):5647-5650.
46. Sijen T*, et al.* (2001) On the role of RNA amplification in dsRNA-triggered gene silencing. *Cell* 107(4):465-476.
47. Vaistij FE, Jones L, & Baulcombe DC (2002) Spreading of RNA targeting and DNA methylation in RNA silencing requires transcription of the target gene and a putative RNA-dependent RNA polymerase. *Plant Cell* 14(4):857-867.
48. Ameres SL*, et al.* (2010) Target RNA-directed trimming and tailing of small silencing RNAs. *Science* 328(5985):1534-1539.
49. Baccarini A*, et al.* (2011) Kinetic analysis reveals the fate of a microRNA following target regulation in mammalian cells. *Curr Biol* 21(5):369-376.
50. Chung IK*, et al.* (1998) Generation of the short RNA transcript in *Leishmaniavirus* correlates with the growth of its parasite host, *Leishmania*. *Molecules and cells* 8(1):54-61.
51. Livak KJ & Schmittgen TD (2001) Analysis of relative gene expression data using real-time quantitative PCR and the 2(-Delta Delta C(T)) Method. *Methods* 25(4):402-408.
52. Wu Q, Wang X, & Ding SW (2010) Viral suppressors of RNA-based viral immunity: host targets. *Cell Host Microbe* 8(1):12-15.
53. Chiba S & Suzuki N (2015) Highly activated RNA silencing via strong induction of dicer by one virus can interfere with the replication of an unrelated virus. *Proc Natl Acad Sci U S A* 112(35):E4911-4918.
54. Galiana-Arnoux D, Dostert C, Schneemann A, Hoffmann Ja, & Imler J-L (2006) Essential function in vivo for Dicer-2 in host defense against RNA viruses in drosophila. *Nature immunology* 7(6):590-597.
55. Lambrechts L*, et al.* (2013) Specificity of resistance to dengue virus isolates is associated with genotypes of the mosquito antiviral gene Dicer-2. *Proc Biol Sci* 280(1751):20122437.
56. Rodriguez-Cousino N, Gomez P, & Esteban R (2013) L-A-lus, a new variant of the L-A totivirus found in wine yeasts with Klus killer toxin-encoding Mlus double-stranded RNA: possible role of killer toxin-encoding satellite RNAs in the evolution of their helper viruses. *Appl Environ Microbiol* 79(15):4661-4674.

57. Wickner RB & Edskes HK (2015) Yeast killer elements hold their hosts hostage. *PLoS Genet* 11(5):e1005139.
58. Wang AL & Wang CC (1991) Viruses of the protozoa. *Annu Rev Microbiol* 45:251-263.
59. el-Sherbeini M & Bostian KA (1987) Viruses in fungi: infection of yeast with the K1 and K2 killer viruses. *Proc Natl Acad Sci USA* 84(12):4293-4297.
60. Fink GR & Styles CA (1972) Curing of a killer factor in *Saccharomyces cerevisiae*. *Proc Natl Acad Sci U S A* 69(10):2846-2849.
61. Redmond S, Vadivelu J, & Field MC (2003) RNAit: an automated web-based tool for the selection of RNAi targets in *Trypanosoma brucei*. *Molecular and Biochemical Parasitology* 128(1):115-118.
62. Robinson KA & Beverley SM (2003) Improvements in transfection efficiency and tests of RNA interference (RNAi) approaches in the protozoan parasite *Leishmania*. *Mol Biochem Parasitol* 128(2):217-228.
63. Peacock CS*, et al.* (2007) Comparative genomic analysis of three *Leishmania* species that cause diverse human disease. *Nature Genetics* 39(7):839-847.
64. Adams MJ, Lefkowitz EJ, King AM, & Carstens EB (2014) Ratification vote on taxonomic proposals to the International Committee on Taxonomy of Viruses (2014). *Arch Virol* 159(10):2831-2841.

Figure Legends

Figure 1: Properties of *Lbr* siRNAs and sRNAs from *Lbr* and *Lgy*.

A) Distributions of read lengths of siRNAs or sRNAs mapping to *Leishmania* genomes or LRV1s. Shown are 1) AGO1-bound siRNAs (black, solid) or sRNAs (black, dashed) from WT *Lbr* M2903 mapping to the *Lbr* genome, 2) *Lgy* M4147 sRNAs mapped to the *Lg* genome (blue, solid) or LRV1-LgyM4147 (blue, dashed), and 3) *Lbr* LEM2780 sRNAs mapped to the *Lbr* genome (green, solid) or LRV1-LbrLEM2780 (green, dashed). B) Percentage of 23 nt sRNA reads (20-26nt) mapping to transposable elements (TEs, white), rRNA (red), tRNAs (black), genomic repeat regions (yellow), LRV1 (purple), and other *Leishmania* genomic regions (other, gray).

Figure 2: RNAi constructs for LRV1 elimination.

A) Schematic of an RNAi "stem-loop" (StL) construct. Each construct includes an inverted repeated sequence containing 800-1200 bp of the target gene (gene of interest, GOI) and a hygromycin drug resistance marker (HYG^R). The construct is flanked with sequence of the small subunit ribosomal RNA gene, which allows it to integrate into this locus, where it is transcribed at high levels. Splice acceptor (SA) signals within the construct allow for polyadenylylation and processing.

B) Schematic showing LRV1 genome organization and regions targeted for RNAi StL constructions (thick bars) from *Lbr* LEM2700, LEM2780, and LEM3874, and *Lgy* M4147 targeted by RNAi (white, capsid; gray, RDRP). The locations of qPCR amplicons for quantification of LRV1 levels are shown (thin black bars).

Figure 3: Loss of LRV1 induced by RNAi

Anti-capsid flow cytometry analysis of LRV1-knockdown lines in *Lgy* M4147 and *Lbr* LEM2780 (top and bottom panels respectively). LRV1 capsid protein levels are unchanged in GFP65 StL lines, while LRV1 StL lines have undetectable capsid protein. Red, parent lines; purple, GFP65 StLs (off target control); green, LRV1-negative controls; light blue, Capsid StL; dark blue, RDRP StL.

Figure 4. Overexpression of LRV1-mapping 23 nt sRNAs in LRV1 StL transfectants.

A) Genomic mapping of 23 nt sRNA reads from sRNA sequencing of parental or capsid StL *Lgy* M4147 (left) or capsid-RDRP StL *Lbr* LEM3874 (right) mapping to transposable elements (TEs, white), rRNA (red), tRNAs (black), genomic repeat regions (yellow), LRV1 (purple), and other *Leishmania* genomic regions (other, gray). B) LRV1 mapping of 23 nt sRNA reads from LRV1StL lines described in panel A (*Lgy* M4147, top; *Lbr* LEM3874, bottom). Light gray trace indicates parental read distributions; dark gray trace indicates LRV1 StL read distributions. The dark box indicates the region targeted by the StL stems.

Figure 5: The LRV1 genome is completely lost in most LRV1-StL transfectants

qPCR analysis of LRV1 RNA levels in LRV1 StL transfectant clones of *Lbr* LEM2700 (A) and *Lgy* M4147 (B), along with positive and negative controls (+ and – respectively) and control GFP65 StL transfectants. White bars denote a non-specific qPCR product, while black bars denote an LRV1-specific amplicons (melt curve analysis). Dashed line indicates cutoff for designating a clone as LRV1-negative. Error bars are the standard deviation of three technical replicates for each line.

Figure 6. LRV1 elimination results in decreased release of cytokines from infected macrophages.

TNF-α or IL-6 levels were quantified 24h after infection of macrophages with *Lb*r LEM2780 (A) or *Lg* M4147 (B) parent, GFP65 knockdown control, or LRV1-StL transfectants. In both studies the LRV1-control was *Lgy* M4147. For A, results are averages of two-three technical replicates for two clones of each line. For B, results are the averages of two technical replicates for three to six clones of each line. NS, not significant; ** $p < 0.01$; *** $p < 0.0001$ by t-test.

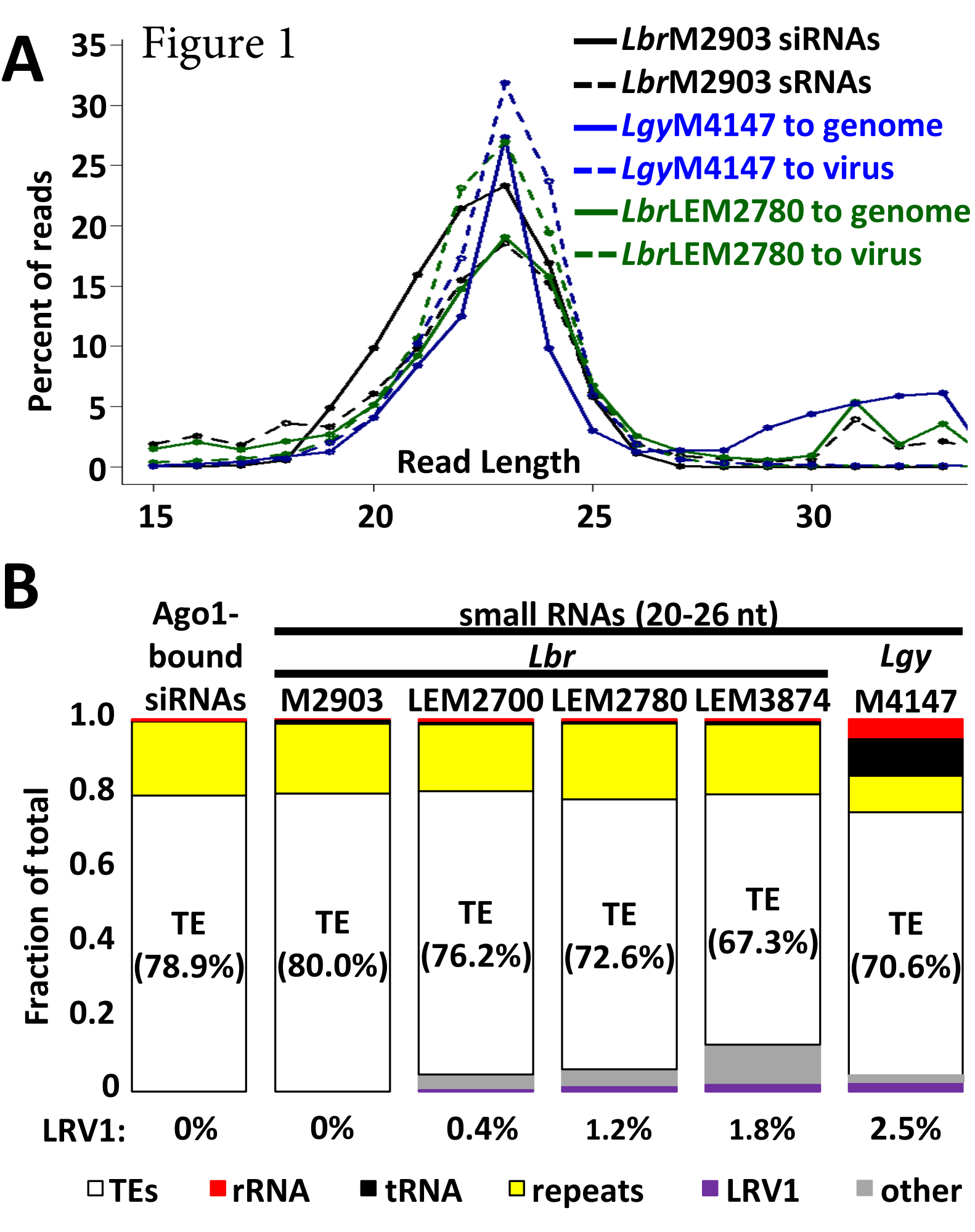
Figure 1
A
Percent of reads
Read Length
LbrM2903 siRNAs
LbrM2903 sRNAs
LgyM4147 to genome
LgyM4147 to virus
LbrLEM2780 to genome
LbrLEM2780 to virus
B
Ago1-bound siRNAs
small RNAs (20-26 nt)
Lbr
Lgy
M2903
LEM2700
LEM2780
LEM3874
M4147
Fraction of total
TE (78.9%)
TE (80.0%)
TE (76.2%)
TE (72.6%)
TE (67.3%)
TE (70.6%)
LRV1: 0% 0% 0.4% 1.2% 1.8% 2.5%
TEs
rRNA
tRNA
repeats
LRV1
other

Figure 2

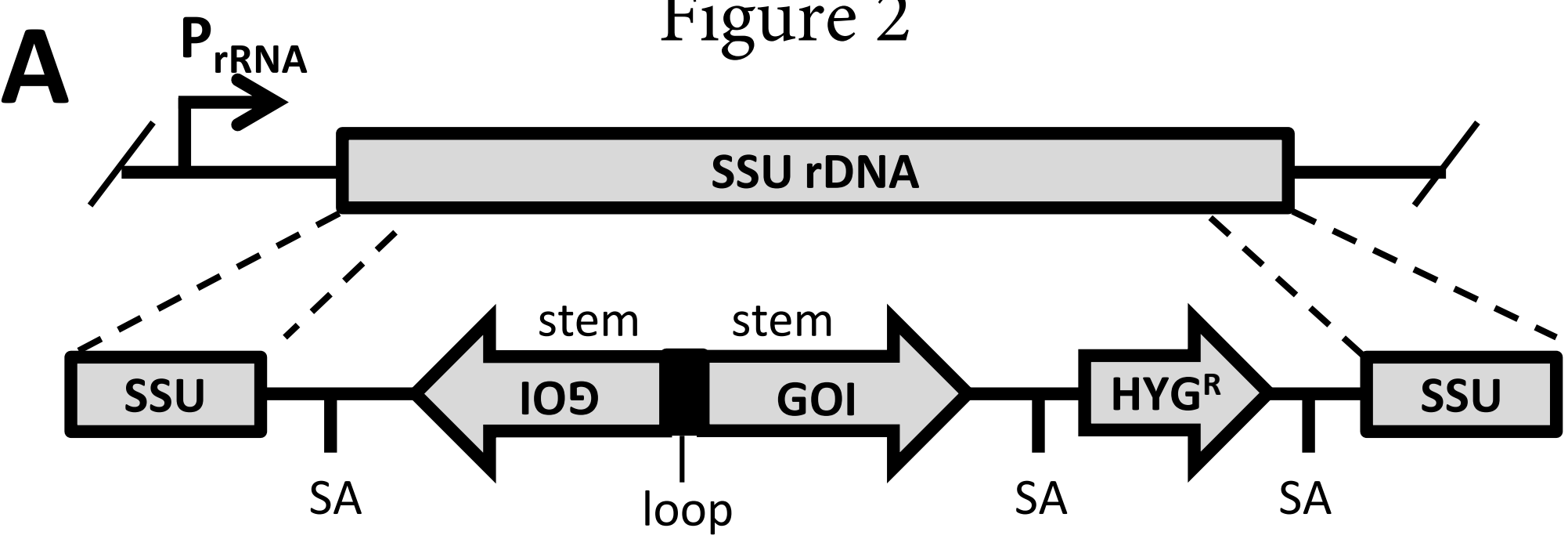
A
P rRNA
SSU rDNA
stem
stem
SSU
GOI
GOI
HYG R
SSU
SA
loop
SA
SA

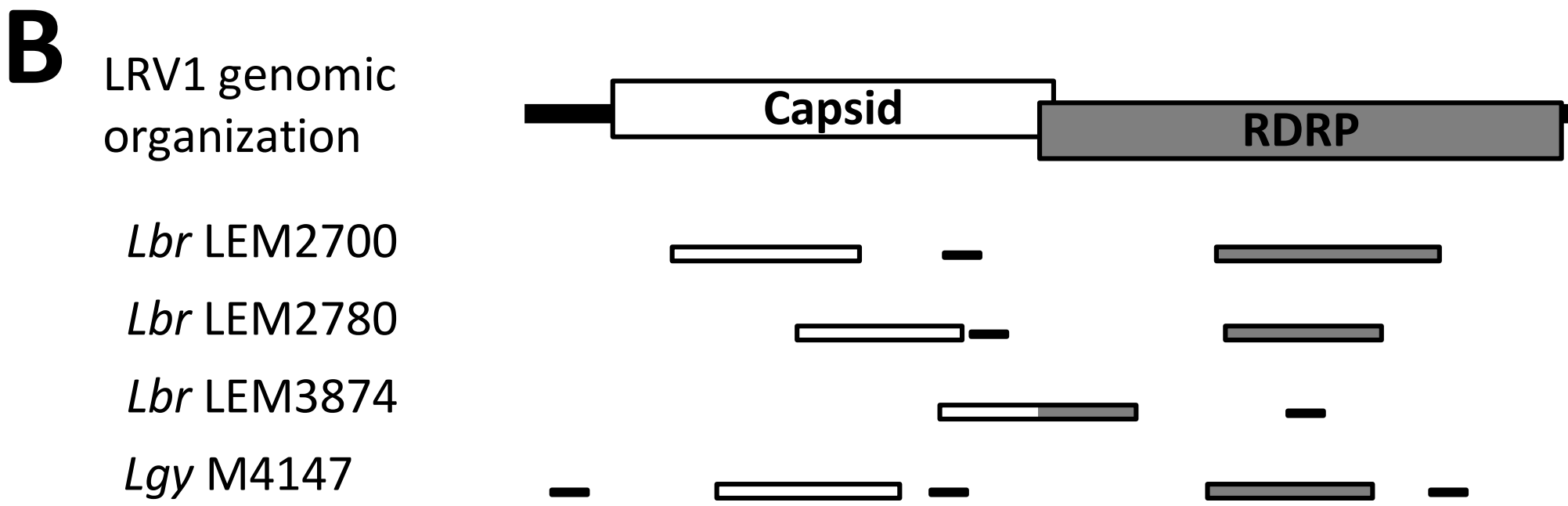
B
LRV1 genomic organization
Capsid
RDRP
Lbr LEM2700
Lbr LEM2780
Lbr LEM3874
Lgy M4147

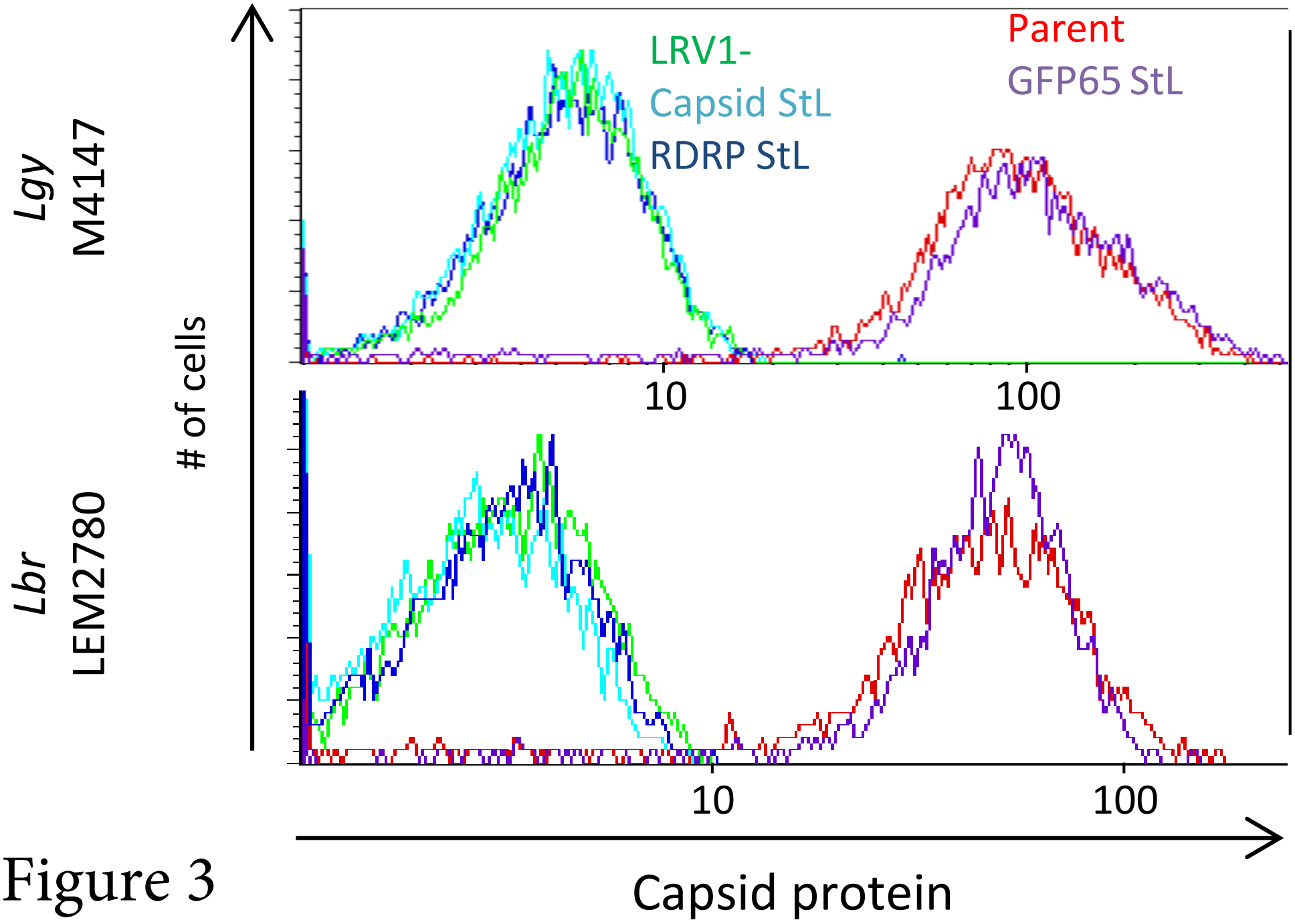
Lgy
M4147
Lbr
LEM2780
# of cells
LRV1-
Capsid StL
RDRP StL
Parent
GFP65 StL
10
100
10
100
Capsid protein

Figure 3

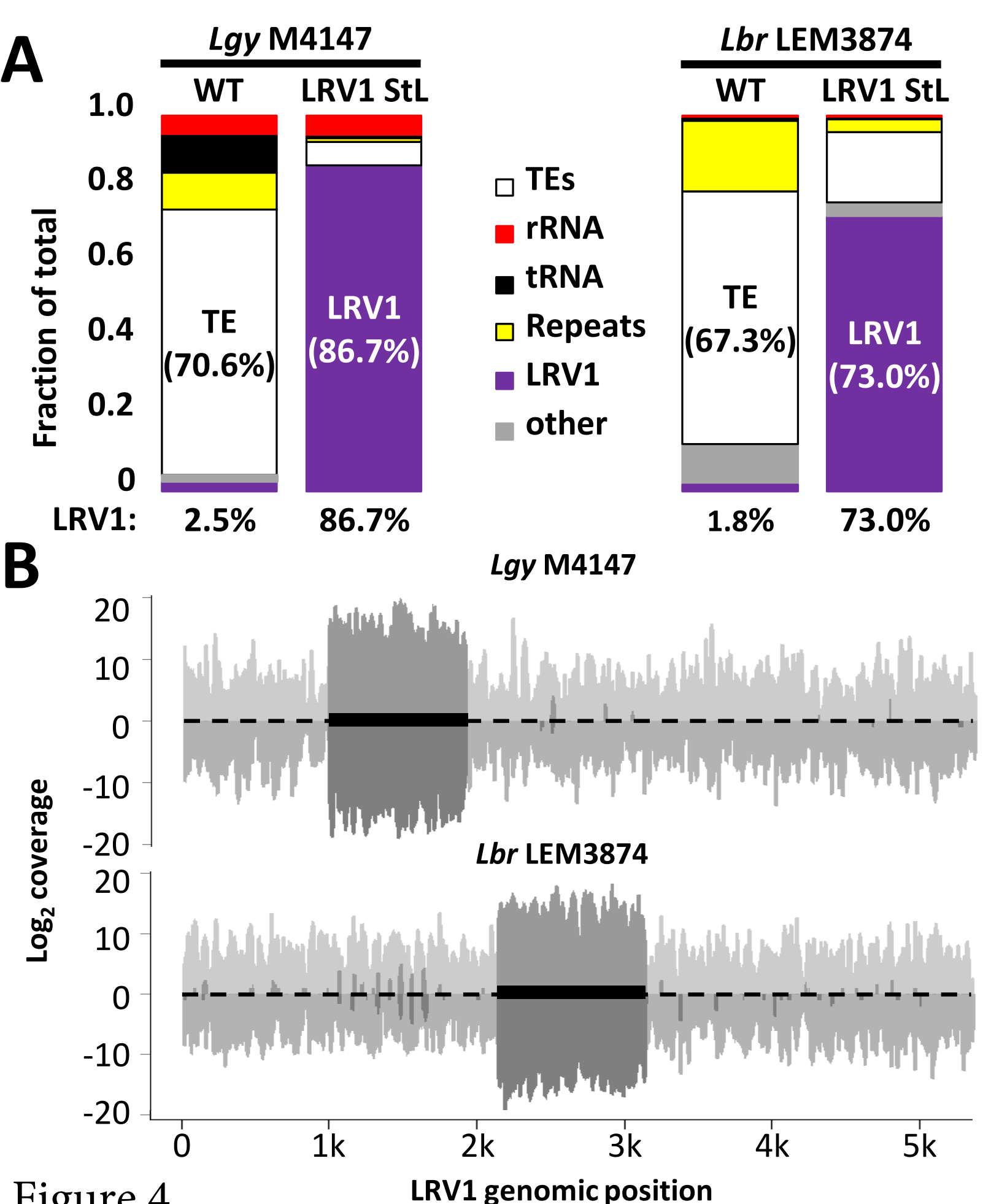
A
Lgy M4147
Lbr LEM3874
WT
LRV1 StL
WT
LRV1 StL
1.0
0.8
0.6
0.4
0.2
0
Fraction of total
TE
(70.6%)
LRV1
(86.7%)
TE
(67.3%)
LRV1
(73.0%)
TEs
rRNA
tRNA
Repeats
LRV1
other
LRV1:
2.5%
86.7%
1.8%
73.0%
B
Lgy M4147
Lbr LEM3874
20
10
0
-10
-20
Log2 coverage
0
1k
2k
3k
4k
5k
LRV1 genomic position

Figure 4

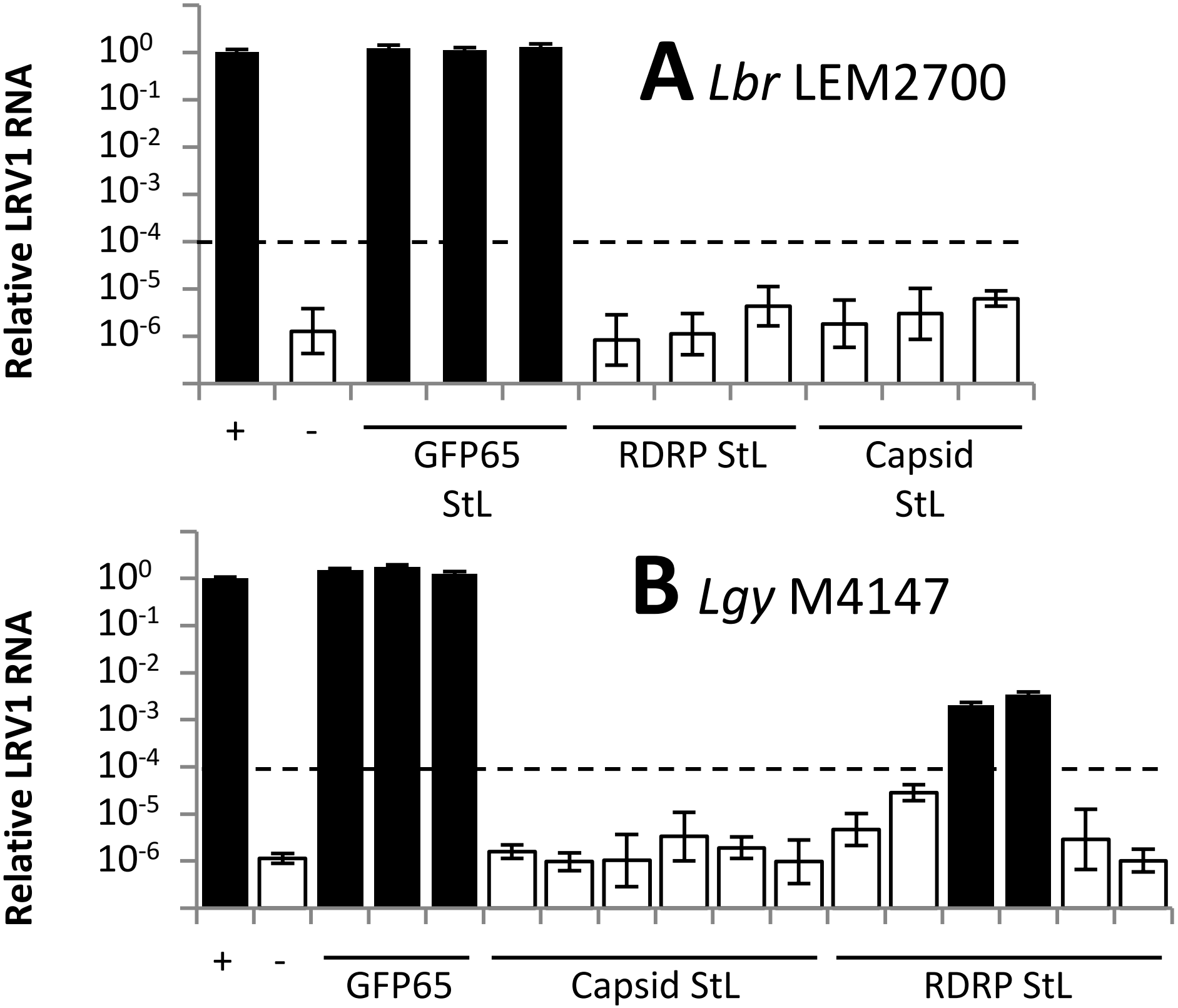
A Lbr LEM2700
Relative LRV1 RNA
10^0
10^-1
10^-2
10^-3
10^-4
10^-5
10^-6
+
-
GFP65 StL
RDRP StL
Capsid StL
B Lgy M4147
Relative LRV1 RNA
10^0
10^-1
10^-2
10^-3
10^-4
10^-5
10^-6
+
-
GFP65 StL
Capsid StL
RDRP StL

Figure 5

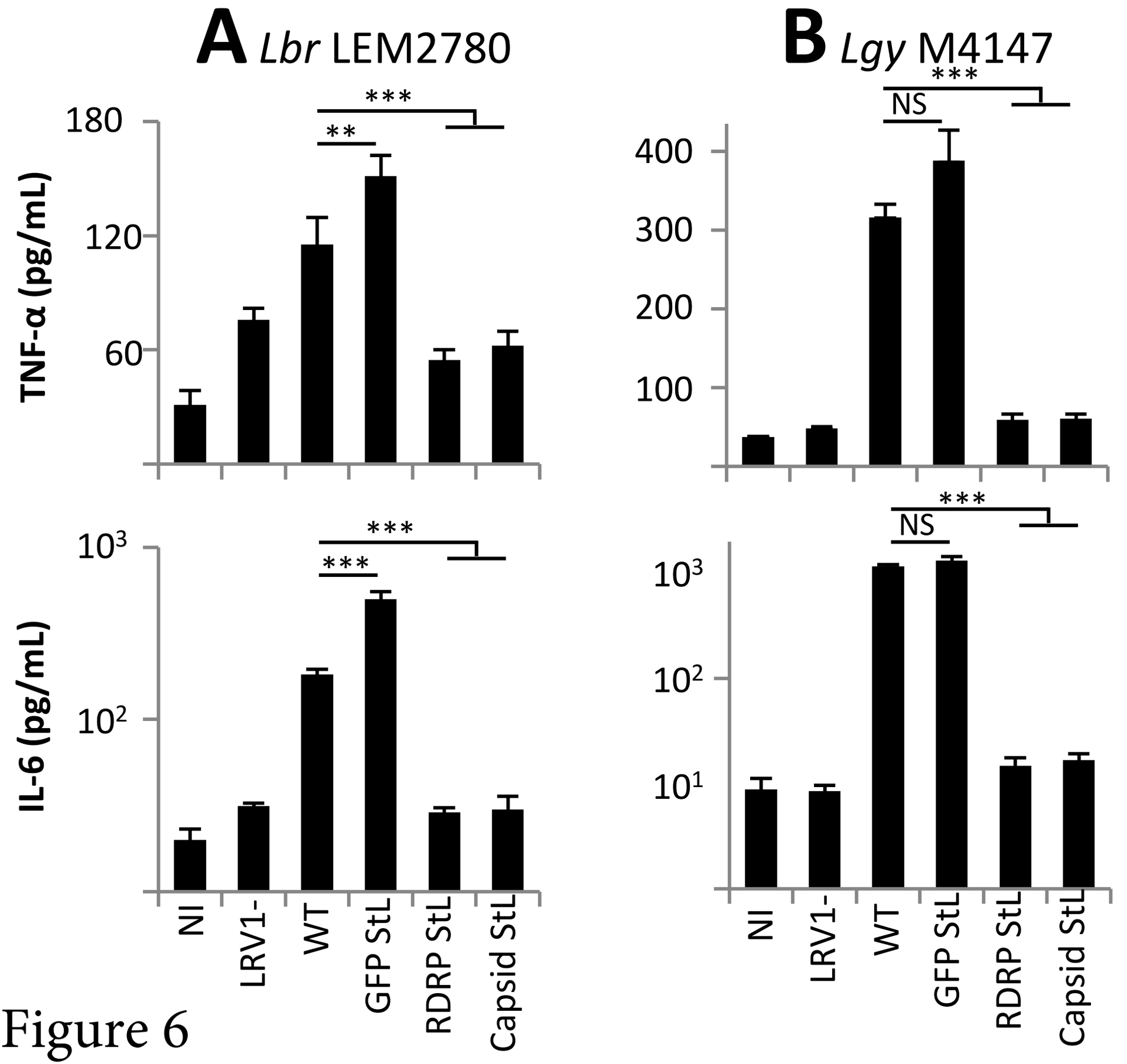
A Lbr LEM2780
B Lgy M4147
TNF-α (pg/mL)
IL-6 (pg/mL)
180
120
60
400
300
200
100
10^3
10^2
10^1
***
**
NS
NI
LRV1-
WT
GFP StL
RDRP StL
Capsid StL

Figure 6

Supplementary Information

Supplemental Table Legends

Table S1: 23 nt siRNA analysis to *Leishmania* genome and LRV1. For *Lbr*, *Lbr* M2904 reference genome was used, and for *Lgy*, a M4147 draft genome (BioProject PRJEB168, accession numbers HG800646-HG802771) was used. References for viral genomes are sequences reported in this work.

Table S2: Distributions of reads mapped to *Lbr* and *Lgy* genomes for Ago1-bound siRNAs, 23 nt (20-26 nt) and 33 nt (30-36 nt) sRNAs.

Table S3: Primer sequences used to amplify regions of LRV1 for cloning into stem-loop constructs.

Table S4: Primer sequences used to measure LRV1 RNA levels by qPCR.

Supplemental Figure Legends

Supplemental Figure 1: Properties of *Lbr* siRNAs and 23 nt sRNAs from *Lbr* and *Lgy*.

This figure shows mapping of the indicated small RNAs after 'collapsing' the data to remove duplicate reads. Shown are the percentages of 23 nt sRNA reads (20-26nt) mapping to transposable elements (TEs, white), rRNA (red), tRNAs (black), genomic repeat regions (yellow), LRV1 (purple), and other Leishmania genomic regions (other, gray). A) As in Figure 1B, mappings in WT parent lines. B) As in Figure 4A, comparing parental lines with capsid StL *Lgy* M4147 (left) or capsid-RDRP StL *Lbr* LEM3874 (right).

Supplemental Figure S2: Mapping of 23nt sRNA reads (20-26 nt) from the respective parasite lines to LRV1-LbrLEM2700 (A), LRV1-LbrLEM2780(b) (B), LRV1-LbrLEM3874 (C), and LRV1-LgyM4147 (D). Reads mapping to the positive strand, (light gray); negative strand, (dark gray).

Supplemental Figure S3: Capsid protein is lost in *Lgy* M4147 capsid StL transfectants.

Three GFP65 StL control clones and six Capsid StL clones were evaluated. Top panel: Western blot analysis was performed using g018d53 anti-capsid polyclonal antibody (35). The arrow marks the location of the capsid protein band. Bottom panel: Ponceau S stain of protein gel.

Supplemental Figure S4: qPCR analysis of LRV1 RNA levels in LRV1 StL clones of *L. braziliensis* strain LEM2780 (A), *L. braziliensis* strain LEM3874 (B), and re-cloned *L. guyanensis* M4147 RDRP StL c3 (C).

White bars denote a non-specific product; black bars denote an LRV1-specific product (melt curve analysis). Dashed line indicates cutoff for designating a clone as LRV1-negative. Error bars are the standard deviation of three technical replicates for each line.

Supplemental Figure S5: Infection of macrophages by *Lbr* LEM2700 (A) and *Lgy* M4147 (B).

TNF-α or IL-6 levels were quantified 24h after infection of macrophages with *Lbr* (A) or *Lgy* (B) parasites. NI, not infected; LRV1+ or LRV1-, infected with *Lgy* M4147 LRV1+ or LRV1-negative cells; GFP65 StL transfectants; and RDRP StL or capsid StL transfectants. A) Results are the averages of two technical replicates of two clones per line. Dark gray bars, experiment performed using WT macrophages; light gray bars, experiment performed using TLR3 knockout macrophages. B) Results are the averages of two technical replicates for each representative clone indicated. Lines found to be LRV1+ by qPCR are denoted by black bars; white bars are lines found to be LRV1-negative by qPCR.

Table S1: Summary of sRNA reads and mapping

A. Total Reads.

Sample	Total reads (raw)	Total Trimmed Reads aligned to the *Leish.* genomes + viruses (Percent total)	Aligned 33 nt peak reads to *Leishmania* (% alignable reads)	Aligned 23 nt peak reads to *Leishmania* (% alignable reads)	Aligned 23 nt peak reads to LRV1 (% alignable reads)	Percent with 3' extension (*Leishmania*)	Percent with 3' extension (LRV1)	Genome-mapping reads 3' extension base A-T-C-G (%)
Lbr M2903[a]	29,391,347	19,447,509 (66.2%)	1,827,623 (9.40 %)	15,147,603 (77.9 %)	n/a	21	n/a	43-41-8-8
Lbr LEM2700	40,384,483	29,473,443 (73.0%)	8,055,506 (27.3%)	15,540,670 (52.7%)	59,287 (0.20%)	19	20	43-41-7.9-8.1
Lbr LEM2780[b]	48,615,815	34,959,518 (71.9%)	5,121,894 (14.7%)	25,361,713 (72.5%)	326,021 (0.93%)	20	20	43-40-7.8-8.2
Lbr LEM3874	36,543,649	25,591,362 (70.0%)	4,052,707 (15.8%)	16,756,188 (65.5%)	347,022 (1.36%)	19	19	44-41-6.6-7.4
Lgy M4147	55,220,664	37,159,548 (67.3%)	1,261,927 (3.40 %)	25,489,186 (68.6 %)	660,143 (1.78%)	15	13	32-33-19-15

B. Collapsed Reads

Sample	Total reads (raw)	Total Trimmed Reads aligned to the *Leish.* genomes + viruses	Aligned 33 nt peak reads to *Leishmania* (% alignable reads)	Aligned 23 nt peak reads to *Leishmania* (% alignable reads)	Aligned 23 nt peak reads to LRV1 (% 23 nt reads)	Percent with 3' extension (*Leishmania*)	Percent with 3' extension (LRV1)	Genome-mapping reads 3' extension base A-T-C-G (%)
Lbr M2903[a]	2,327,188	1,038,131 (44.6%)	68,895 (6.64%)	776,204 (74.8 %)	n/a	37	n/a	35-35-15-15
Lbr LEM2700	2,948,017	1,206,587 (40.9%)	127,998 (10.6%)	758,664 (62.9 %)	18,642 (1.54%)	35	36	34-34-16-16
Lbr LEM2780[b]	3,439,169	1,777,142 (51.7%)	150,229 (8.45%)	1,050,094 (59.1 %)	61,753 (3.47%)	33	34	34-34-16-16
Lbr LEM3874	2,379,761	1,224,741 (51.5%)	105,696 (8.63%)	632,961 (51.7%)	48,287 (3.94%)	31	32	35-35-15-15
Lgy M4147	1,437,673	752,464 (52.3%)	152,059 (20.2%)	358,039 (47.6%)	43,099 (5.73%)	22	22	30-28-22-20

[a] *Lbr* M2903 SSU:IR2-LUCSR. [b] The sum of reads mapping to LRV1-LbrLEM2780(a) and (b) are shown, which map quantitatively to similar levels.

Table S2. Genomic mapping of 23 and 33 nt 'peak' sRNA fractions from *Lbr* and *Lgy*.

	Lbr M2903			*Lgy* M4147	
	AGO1-bound siRNAs	**23 nt (20-26 nt) sRNAs**	**33 nt (30-36 nt) sRNAs**	**23 nt (20-26 nt) sRNAs**	**33 nt (30-36 nt) sRNAs**
Alignable reads	20,029,304	19,447,509	1,827,623	37,159,548	1,261,927
Percent mapping to:					
Transposable elements					
SLACS	33.9	26.9	1.2	59.8	0.25
TATE	45.1	53.1	5.2	10.7	0.32
Repeats					
Misc.	5.8	5.0	7.7	1.1	2.4
TAR	4.7	4.2	0.08	4.0	0.38
TAS	4.2	5.1	20.3	4.8	6.5
CIR	5.1	4.6	0.09	0.0	0.0
Structural RNAs					
tRNAs	0.12	0.75	32.1	9.9	75.4
rRNAs	0.42	0.47	29.4	5.5	14.6

Transposable elements, repeats and structural RNAs were classified as defined in the Methods and by Atayede *et al* (26)

Table S3: Primer sequences used to amplify regions of LRV1 for cloning into stem-loop (StL) constructs.

Parasite strain	Target	Construct ID	Name	Stem length	Sequence - is the border or the oligo? Some look like one some the other
Lbr LEM2700	Capsid	B6910	pIR2HYG-LRV1_LbrLEM2700_CapsidStL(A)	943 bp	5'-CGCTAGTCTAGAATACTACAGCAAACATGTTTCG
					5'-CGCTAGTCTAGACAAGGTGTCTGTTGGGTTCGAT
	RDRP	B6908	pIR2HYG-LRV1_LbrLEM2700_RDRPStL(A)	1143 bp	5'-CGCTAGTCTAGAATGTGCTTCAAACTTGAAGATG
					5'-CGCTAGTCTAGATAGCAGCAATCTAACGACCTGC
Lbr LEM2780	Capsid	B7061	pIR2HYG-LRV1_LbrLEM2780_CapsidStL(A)	835 bp	5'-CCAGCTTGGGATCAATTTGCGG
					5'-GGACATCTCCATCAGCCGATGA
	RDRP	B7062	pIR2HYG-LRV1_LbrLEM2780_RDRPStL(A)	794 bp	5'-GTGAGGATGAGTTGCGCGCTGC
					5'-ATTGCTAAGTAGACTGTTTGCG
Lbr LEM3874	Capsid / RDRP	B7268	pIR2HYG-LRV1_LbrLEM3874_StL(A)	1000 bp	5'-GGCTAGTCTAGA GTCGTGCGATCTATTCCATCCT
					5'-GGCTAGTCTAGATTAGTGCTTATGTTAGGATCAG
Lgy M4147	Capsid	B7066	pIR2HYG-LRV1_LgyM4147_CapsidStL(A)	926 bp	5'-CTTCTCCTTTACGTGCCAGC
					5'-GCGCATTGTTGTCCACTCAA
	RDRP	B7063	pIR2HYG-LRV1_LgyM4147_RDRPStL(A)	829 bp	5'-CTTGCTAGGTCGTGGGGTGA
					5'-ACCAACATGCATAGACGTGG

Table S4: Primer sequences used in measurement of LRV1 RNA levels by qRT-PCR.

KMP-11	F	5’-GCCTGGATGAGGAGTTCAACA
	R	5’-GTGCTCCTTCATCTCGGG
L. braziliensis LEM2700	F	5’-CATCCTGCTGAGTTGACTTCATAC
	R	5’-GTCACACCTTGTGATGACATTGC
L. braziliensis LEM2780	F	5’-GTCATTACGAGGTGTGATGGAAT
	R	5’-GGTAACGCGCCATCACACAGT
L. braziliensis LEM3874	F	5’-GAATATGCTCTCCGACCGGTTG
	R	5’-AATTCTCGCAGCCACCCCACAG
L. guyanensis M4147	Set 1 F	5’-CTGACTGGACGGGGGGTAAT
	Set 1 R	5’-CAAAACACTCCCTTACGC
	Set 2 F	5’-CACGCTAGATGAGTACATCTGG
	Set 2 R	5’-GTAGTTGCGGAATCTGACG
	Set 3 F	5’-GGTAATATCACGCAGTGTAAGC
	Set 3 R	5’-GACACCACCTCTAAGACACG

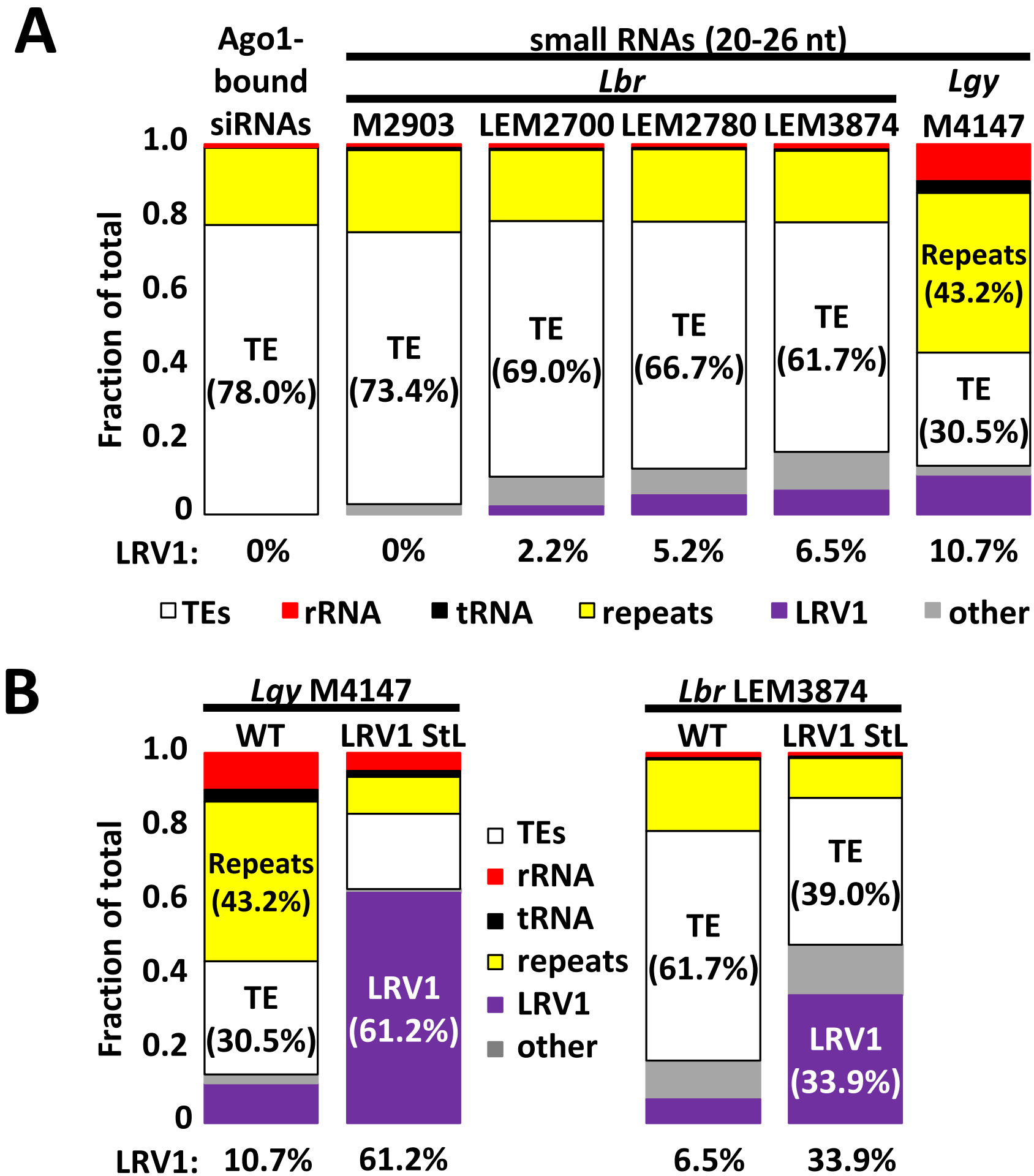
A
Ago1-bound siRNAs
small RNAs (20-26 nt)
Lbr
Lgy
M2903
LEM2700
LEM2780
LEM3874
M4147
Fraction of total
1.0
0.8
0.6
0.4
0.2
0
TE (78.0%)
TE (73.4%)
TE (69.0%)
TE (66.7%)
TE (61.7%)
Repeats (43.2%)
TE (30.5%)
LRV1: 0% 0% 2.2% 5.2% 6.5% 10.7%
TEs
rRNA
tRNA
repeats
LRV1
other
B
Lgy M4147
Lbr LEM3874
WT
LRV1 StL
WT
LRV1 StL
Fraction of total
Repeats (43.2%)
TE (30.5%)
LRV1 (61.2%)
TE (61.7%)
TE (39.0%)
LRV1 (33.9%)
TEs
rRNA
tRNA
repeats
LRV1
other
LRV1: 10.7% 61.2% 6.5% 33.9%

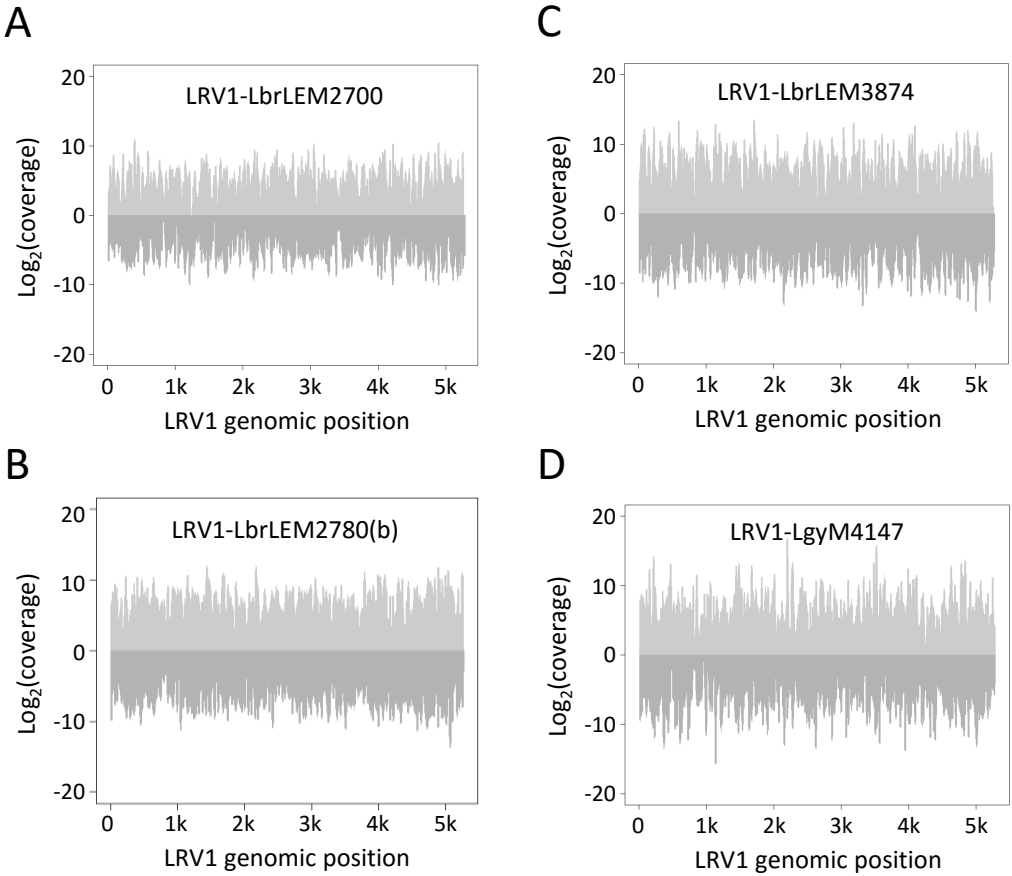
A
LRV1-LbrLEM2700
Log2(coverage)
20
10
0
-10
-20
0
1k
2k
3k
4k
5k
LRV1 genomic position
C
LRV1-LbrLEM3874
Log2(coverage)
LRV1 genomic position
B
LRV1-LbrLEM2780(b)
Log2(coverage)
LRV1 genomic position
D
LRV1-LgyM4147
Log2(coverage)
LRV1 genomic position

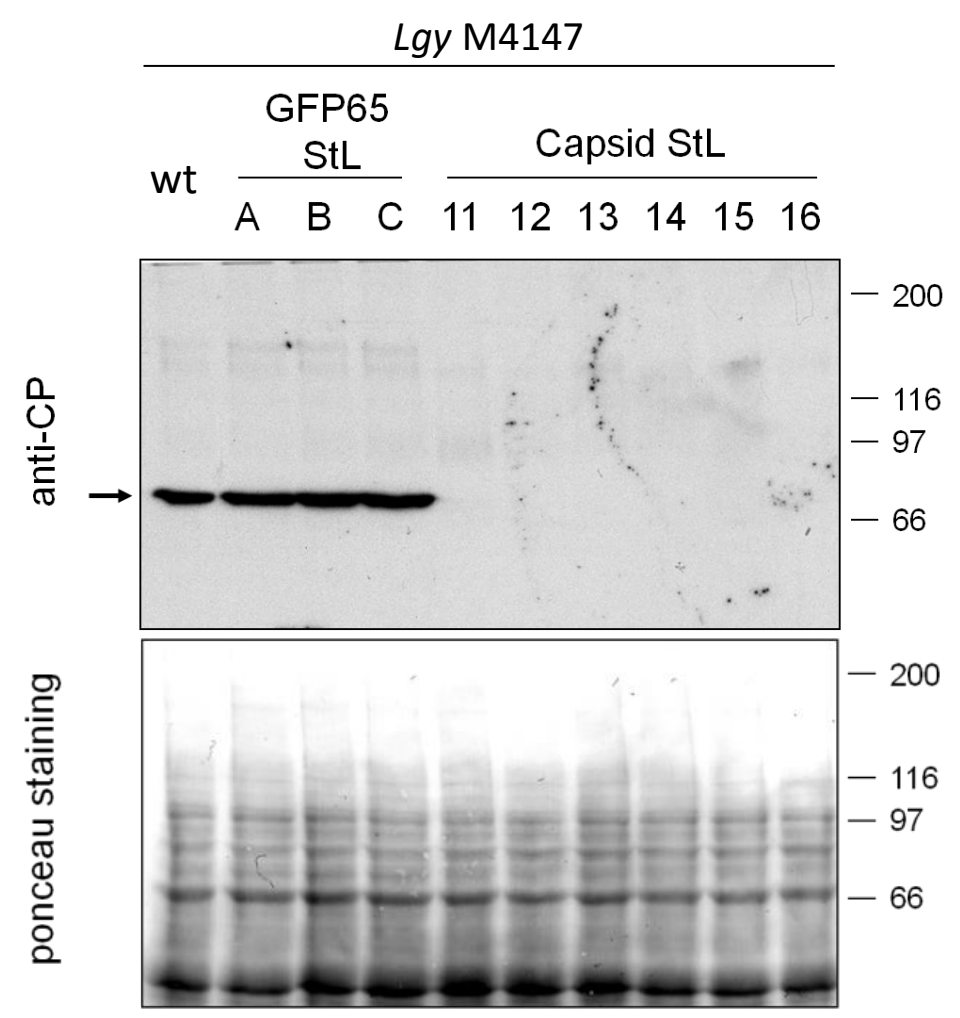
Lgy M4147
wt
GFP65 StL
A
B
C
Capsid StL
11
12
13
14
15
16
anti-CP
200
116
97
66
ponceau staining
200
116
97
66

A. *Lbr* LEM2780

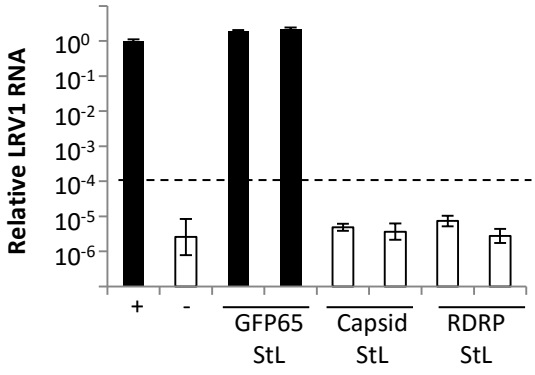

B. *Lbr* LEM3874

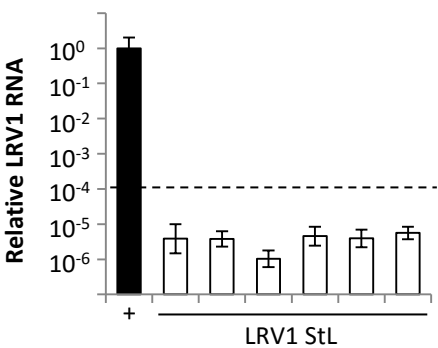

C. *Lgy* M4147 RDRPStL c3 re-cloned

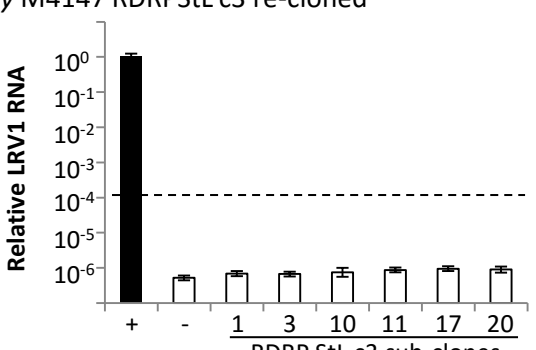

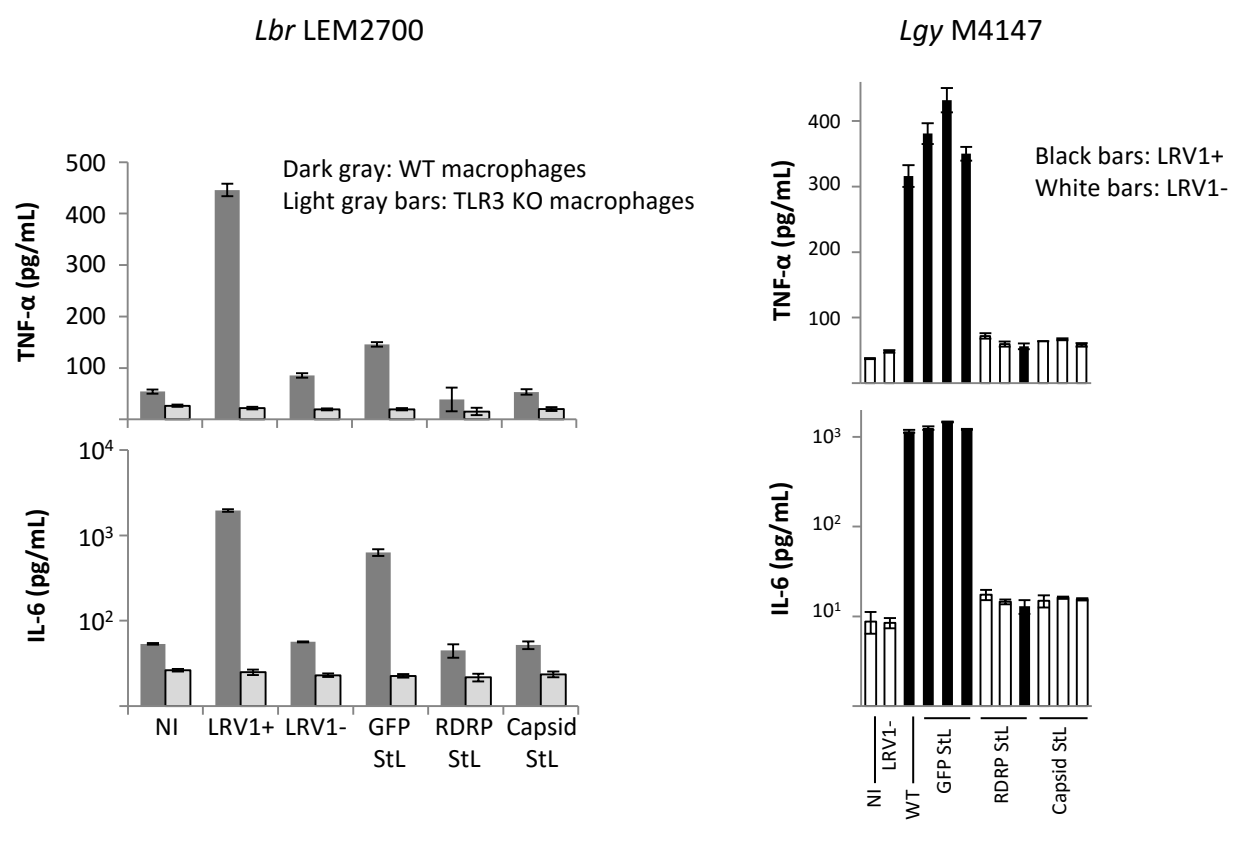
Lbr LEM2700
Dark gray: WT macrophages
Light gray bars: TLR3 KO macrophages
TNF-α (pg/mL)
500
400
300
200
100
IL-6 (pg/mL)
10^4
10^3
10^2
NI
LRV1+
LRV1-
GFP StL
RDRP StL
Capsid StL
Lgy M4147
Black bars: LRV1+
White bars: LRV1-
TNF-α (pg/mL)
400
300
200
100
IL-6 (pg/mL)
10^3
10^2
10^1
NI
LRV1-
WT
GFP StL
RDRP StL
Capsid StL